University of Stavanger

Faculty of Science and Technology

MASTER'S THESIS

Study program/ Specialization: Petroleum Technology - Reservoir	Spring semester, 2017 Open / Restricted access
Writer: Kevin Jørgensen	…… (Writer'ssignature)
Faculty supervisor: Dag Chun Standnes External supervisor(s):	
Thesis title: A study of the diffusion coefficient term in counter current imbibition and its effect on production	
Credits (ECTS): 30	
Key words: Spontaneous imbibition, counter current flow, non linear diffusion, coefficient term, eclipse 100, core plug	Pages: 75 + enclosure: 25 Stavanger, 14.06.2017 Date/year

Front page for master thesis
Faculty of Science and Technology

Abstract

It is believed that most reservoirs have at least some degree of fractures and spontaneous imbibition is considered to be one of the most important recovery processes in fractured reservoirs. The imbibiton process can be described by a diffusion equation that combines Darcy's law and mass balance, which leads to an expression with a diffusion coefficient $D(S_w)$ that is dependant on water saturation. This diffusion coefficient make up a large part of the variables in the counter current imbibition process.

The diffusion equation is difficult to solve due to it being a non-linear equation and it is therefore of interest to see if it can be changed to a linear diffusion equation by assuming a constant D.

Simulations are done using the eclipse 100 simulator to try to replicate previously performed experiments on core plugs. These simulations are then used to explore the effect of the diffusion coefficient on oil recovery. As the diffusion coefficient is dependant on water it makes the imbibition formula difficult to solve and it is of interest to see how the oil recovery is dependant on the coefficient shape at different water saturations.

Simulation results show that for the diffusion coefficient shape and total area both affect the oil recovery rate and total oil recovery in a given time period.

Acknowledgement

To begin I would like to express my gratitude to some people that have been important in writing this thesis. I would first like to thank Professor Dag Chun Standnes from the University of Stavanger, who proposed the idea of the topic for this thesis and gave valuable feedback and discussing throughout the full semester. I would also thank the University of Stavanger for the opportunity to learn and writing my thesis here. I would also like to thank my family and friends who encouraged and supported me during my full studies.

List of Figures

List of Tables

A study of the diffusion coefficient term in counter current imbibition and its effect on production

Kevin Jørgensen

June 2017

Contents

1 Introduction and aim

Fractures is the most abundant structural feature that is visible in the Earth's upper crust, and it is likely that most reservoirs contains some natural fractures [31]. It is therefore important to know how fractures affects the recovery of oil in a reservoir and to understand what factors that controls the flow and production in a fractured reservoir. The reservoir fluids will flow in the path of least resistance, which in the case of a fractured reservoir is in the fractures. Fractures have a higher permeability than the reservoir matrix which gives the fluids an opportunity to go into a more spacious area where it will have an easier path to flow from the towards the lower pressure area of the reservoir (or the well in a reservoir that is being produced). In order to understand how a reservoir with fractures works on full scale it is important to first see how it works on a small scale. It is therefore necessary to do experiments and note observations on small scale experiments such as flooding of a core plug.

Spontaneous imbibiton is regarded as one of the most important mechanism when it comes to the recovery from fractures in a reservoir [13]. An imbibition process can occur in two ways, co current flow, where the water imbibing travels the same way as the oil being moved, or counter current flow, where the water imbibing travels the opposite way of the oil that is moved. It has previously been derived a mathematical equation that should explain the process of spontaneous imbibition for counter current flow. In this formula there exists a diffusion coefficient that is dependant on the derivative of the capillary pressure with respect to water saturation. The spontaneous imbibiton process is therefore determined as a non-linear diffusion process that is dependant on the water saturation.

When analysing complex equations it is often necessary to implement numerical analysis as in some cases the equations becomes too complex to solve analytically, such is the case for the counter current spontaneous imbibition equation. Eclipse is a simulation tool that uses numerical calculations in order to predict a outcome of certain input parameters for a reservoir. This software uses a range of different input variables for its predictions such as permeability, capillary pressures, relative permeabilities, a grid for the reservoir and much more.

In this thesis it will be attempted to see if there exists a relationship between the diffusion coefficient, in the spontaneous counter current equation, and the production rate (in terms of the magnitude and shape of the coefficient curve). At first a eclipse model will be validated by matching with previously experimental data on cores. Afterwards the same eclipse model will be used in the attempt to find any correlation between the diffusion coefficient and the production rate.

The aim of this study was to:

- Simulate the experimental tests and history match them
- Compare the numerical solutions from Eclipse with the test results
- Calculate the diffusion coefficients and the total area under the curve
- Evaluate if the production curve will stay the same if the area under the diffusion coefficient is kept constant, regardless of the shape
- Evaluate if there exist a relationship with the shape of the diffusion coefficient curve and the production rate
- Analyze what effect the shape and size of the diffusion coefficient curve have on the production curve

2 Theory

2.1 Oil Recovery in fractured reservoirs

A fractured reservoir consists of two different media that can contain fluids: the porous reservoir matrix and the open fractures. In a fractured reservoir the fractures will have a very large permeability compared to the porous matrix. This often leads to the fluids in the fractures moving with a higher velocity than the fluids in the matrix. During water injection the water will find the path of least resistance and due to the difference in permeability the path of least resistance will be in the fractures. This can lead to a problem if the injection water moves through the fractures and bypasses the oil that is still in the matrix. This problem arises when the matrix is oil-wet which results in a porous matrix that will prefer to hold onto the oil and let the water pass by. This will lead to water moving through the fractures, trapping the oil in the porous matrix as can be seen in figure 1

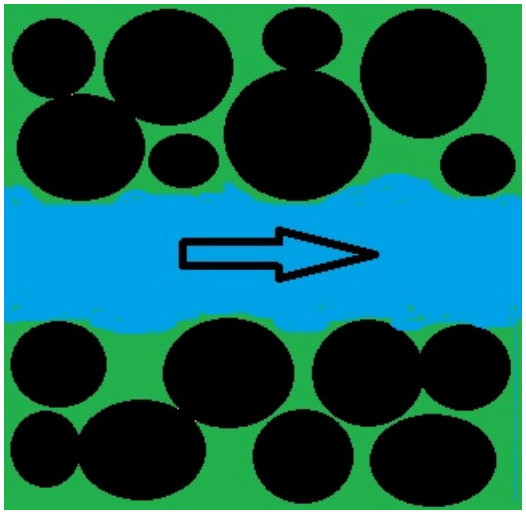

Figure 1: *An illustration of a fracture in the middle of the porous medium where the black dots represents the reservoir matrix. Shows how the (blue) water would bypass the (green) oil in a scenario with oil wet matrix.*

During water injection in a fractured reservoir it is necessary to get the water to move into the pores in the matrix so that it can replace and push out the oil residing in the matrix. One process that allows the water to flow through the pores and replace the oil is called imbibition. If the matrix is water-wet a process called spontaneous imbibition (described in

section 2.2) will occur where the water will force its way into the porous matrix. The water will displace the oil and force the oil to move out of the matrix pores which will result in an increase in oil recovery.

Many fractured reservoirs can experience a high initial oil production from the fractures, but these are often short term effects [12]. These short term effects are experienced due to the fact that the oil in the fractures can move at a higher velocity than the oil in the matrix, and the production rate will decrease as the fractures are depleted of the initial oil and have to wait for the oil in the porous matrix to move into the fractures. After the initial increase in oil recovery has come to an end, the added recovery of oil from the matrix is mostly dependent on spontaneous imbibition which is a relatively slow process [12].

The reservoir rocks are complex structures that often consists of many different types of minerals that each have their wettability preference. In most cases it is not possible to determine one fluid phase to be the only wetting phase for a reservoir matrix due to the complex and homogeneous nature of a reservoir rock. This can lead to a reservoir that is water wet at one place and oil wet at another place. This in turn leads to the possibility of spontaneous imbibition to take place at some parts of the reservoir while in other parts the water in the fractures will bypass and trap the oil. If the reservoir rock is oil wet so that it is not possible for spontaneous imbibition to occur then some form of EOR methods has to be used in order to produce more oil.

2.2 Spontaneous Imbibition

Capillary imbibition is considered to be one of the most important recovery mechanisms in naturally fractured reservoirs, especially for reservoirs where the rock permeability is low. The concept of imbibition involves complex interactions between capillary, gravity and viscous forces [13]. The imbibition forces that are the focus in this thesis will be imbibition due to capillary forces which is also known by the name spontaneous imbibition or natural imbibition [13]. Spontaneous imbibiton is the invasion of one fluid into the porous matrix without the existence of any pressure that is forcing or pushing it into the porous space. In order for spontaneous imbibition to occur the fluid that is invading the matrix has to be the wetting fluid (which will be discussed in section 2.3), otherwise spontaneous imbibition

will not occur. Imbibition can occur in co-current or counter-current flow. In the tests and simulations done in this thesis the imbibition process that occurs is counter-current as it is a fully oil saturated core that is fully immersed in water. Spontaneous imbibition makes it possible to recover oil that can't be recovered by using waterflood as an attempt to develop a pressure gradient that will push oil out.

2.2.1 Co-Current imbibition

Co-Current imbibition is the process of which the non-wetting fluid phase and the wetting fluid phase travels in the same direction during a spontaneous imbibition process. An example for a case like this is a piston like displacement where the wetting phase pushes the non-wetting phase in front of it. An illustration of a piston like displacement can be seen in figure 3.

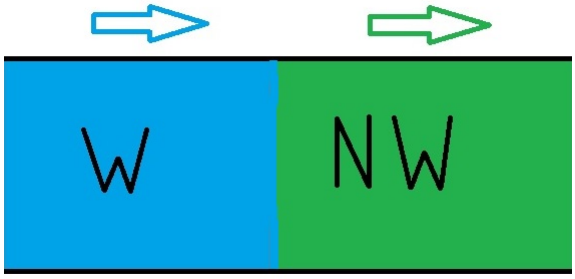

Source:[13]

Figure 2: *An illustration of a co-current imbibition scenario in a water-wet pore where the blue water fluid travels towards the right and pushes the green non-wetting phase, which is then forced to also move to the right.*

An example of conditions where Co-Current imbibition can occur is when there exists multiple fractures. Water in one fracture can in this case imbibe into the matrix, containing oil, and push the oil out and into another fracture.

Co-Current imbibition does not have to deal with the fact that the oil that is being replaced has to move through the same pore space as the imbibing water, as is the case for counter current imbibition, and co-current imbibition tends to move faster than counter current. Usually the rate of a co-current imbibition is about four times as fast as a counter

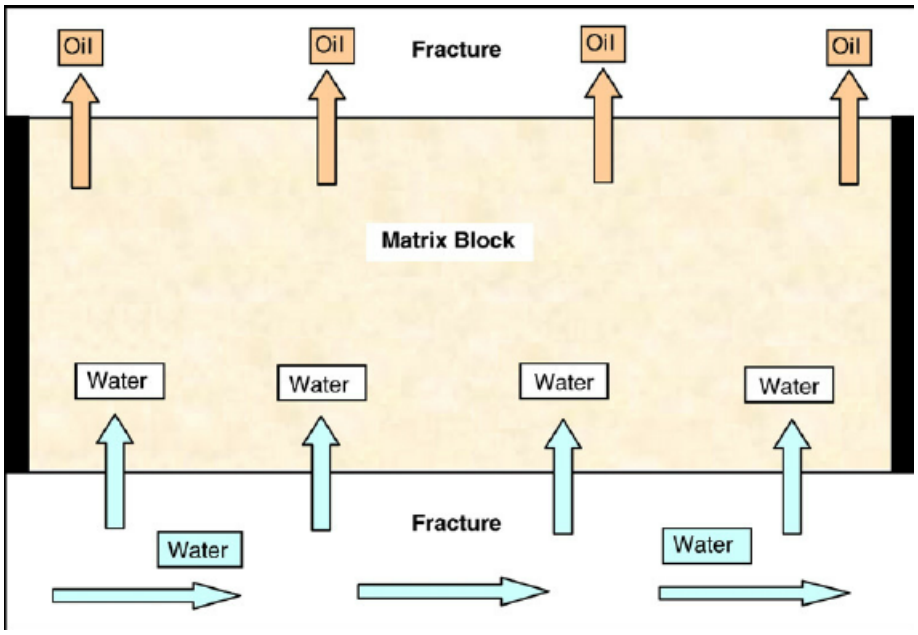

Source:[13]

Figure 3: *An illustration of a co-current imbibition scenario where water from one fracture pushes the oil out into a fracture on the opposite side of the porous matrix.*

current imbibition [17]. Even though the oil recovery seems to be faster for co-current imbibition the total oil recovery was found to be higher for counter-current imbibition [8].

2.2.2 Counter-current imbibition

Counter-current imbibition is the process of which the wetting phase imbibes into porous media and displaces the non wetting phase, in this thesis the water and oil respectively, while the non-wetting phase is forced to move in the opposite direction of the wetting phase. This can occur in a scenario where the non-wetting phase has no other place to move other than where the wetting phase is coming from, such as the case where all fractures in a reservoir is filled with water. This is the case for the tests and simulations in this thesis. A water wet core is saturated with oil and then fully immersed in water with a coated layer on the top and bottom excluding fluid exchange in the top and bottom parts of the core. An illustration of a counter current imbibition flow can be seen in figure 5.

The counter current imbibition process that occurs in the case of a core fully immersed in water is mainly driven by capillary forces, which is discussed later in section 2.5 [9].

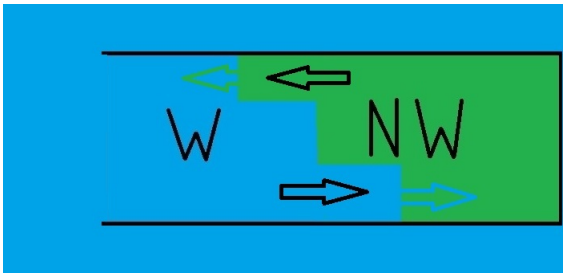

Figure 4: *An illustration of a counter current imbibition scenario in a water-wet pore that is initially filled with oil and surrounded by water. The blue water fluid travels towards and into the porous space while the green oil phase is pushed and forced back in the opposite direction, as indicated by the arrows on top, due to the black no-flow boundaries on the top, bottom and right side.*

This capillary imbibition process allows for recovery of oil that can't be reached by the increased pressure gradient that is applied during a water flood. In the case of a fractured reservoir it has previously been concluded that the capillary imbibition is the main recovery mechanism if the oil is stored in the matrix and a large enough volume of water is given to the fractures [13].

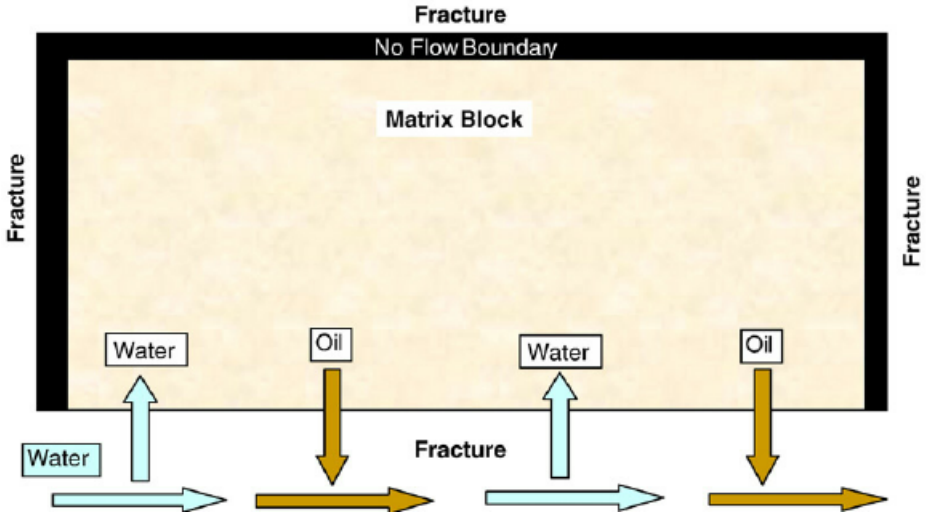

Source: [13]

Figure 5: *An illustration of a counter current imbibition scenario a reservoir where there are no flow boundaries forcing the oil to move in the opposite direction of the imbibing water.*

In this thesis the rate of oil recovery is of interest, and a formula to describe the normalized

oil saturation change in the core has been developed as

$$\phi\frac{\partial S}{\partial t} = \frac{\partial}{\partial x}D(S_w)\frac{\partial S}{\partial x} + \frac{\partial}{\partial y}D(S_w)\frac{\partial S}{\partial y} + \frac{\partial}{\partial z}D(S_w)\frac{\partial S}{\partial z} \tag{1}$$

where

$$D(S_w) = -\frac{Kk_{ro}}{\mu_o}\cdot\frac{1}{1+\frac{k_{ro}}{k_{rw}}\cdot\frac{\mu_w}{\mu_o}}\frac{dP_c}{dS_w} \tag{2}$$

This equation is derived in section 2.2.3 through 2.2.3.3. Here the capillary diffusivity coefficient $D(S_w)$ is a function that is dependant on the water saturation which means that the change in oil saturation and oil recovery is dependant on the water saturation. In this thesis it is of interest to see how the coefficient term affect the oil production and how it changes at different water saturations.

2.2.3 Formulas to derive the imbibition equations

Equation 1 in section 2.2.2 is derived from a few different laws and conditions which will be outlined in this section. The following assumptions and conditions are necessary to derive equation 1 [20]

- incompressible fluids
- volume in is equal to volume out
- constant density

2.2.3.1 Mass balance

In order to get an analytical formula for how the water and oil is exchanged in the core the mass balance equation has to be considered. The mass balance equation consists of three separate parts:

$$\text{Mass in} - \text{Mass out} = \text{Change in mass over time} \tag{3}$$

The mass in and mass out terms in equation 3 can be expressed as

$$\left((uA\rho)(x) - (uA\rho)(x+\Delta x)\right)\Delta t \tag{4}$$

Here the x describes the flow position where x is the in position and $x + \Delta x$ is the flow out position.

In equation 3 the total change in mass can be expressed as

$$(\phi A \Delta x \rho)(t + \Delta t) - (\phi A \Delta x \rho)(t) \tag{5}$$

where the t represents the time and Δt is the change in time.

The mass in minus mass out in equation 4 has to be equal to the total mass change given in equation 5 and it can then be manipulated to a new expression:

$$\begin{gathered} ((uA\rho)(x) - (uA\rho)(x + \Delta x))\Delta t = (\phi A \Delta x \rho)(t + \Delta t) - (\phi A \Delta x \rho)(t) \\ \frac{(uA\rho)(x) - (uA\rho)(x + \Delta x)}{\Delta x} = \frac{(\phi A \rho)(t + \Delta t) - (\phi A \rho)(t)}{\Delta t} \\ -\frac{\partial}{\partial x}(u\rho) = \frac{\partial}{\partial t}(\phi\rho) \\ \frac{\partial}{\partial t}(\phi\rho) + \frac{\partial}{\partial x}(u\rho) = 0 \end{gathered} \tag{6}$$

If it is assumed that it is incompressible fluids and the density is constant then the density term can be divided on both sides of the equation and the expression becomes

$$\phi \frac{\partial}{\partial t} + \frac{\partial}{\partial x} u = 0 \tag{7}$$

2.2.3.2 Darcy's law

Darcy's law is an equation that describes the rate at which a fluid travels from a place of higher potential (pressure) to a position of lower potential. The general equation is given as [21]

$$Q = -\frac{KA}{\mu} \frac{(P(b) - P(a))}{L} \tag{8}$$

Q is the volume flow rate. The $P(b)$ and $P(a)$ refers to the pressure in the end position b and starting position a. The L is the distance between a and b, while K is the absolute permeability and A is the area of which the fluid travels through. μ is the viscosity of the fluid.

The fraction $\frac{(P(b)-P(a))}{L}$ can be written as a derivative when the distance L goes towards zero (as per the definition of a derivative given in section 2.7.1).

$$\begin{aligned} Q &= -\frac{KA}{\mu}\frac{\partial P}{\partial x} \\ u &= -\frac{K}{\mu}\frac{\partial P}{\partial x} \end{aligned} \tag{9}$$

Darcy's law can be considered for both oil flow and water flow. Since the counter-current imbibition case of the core has flow of both oil and water (in opposite directions), both of these equations has to be considered.

$$\begin{aligned} u_o &= -\frac{Kk_{ro}}{\mu_o}\frac{\partial P_o}{\partial x} = -\lambda_o\frac{\partial P_o}{\partial x} \\ u_w &= -\frac{Kk_{rw}}{\mu_w}\frac{\partial P_w}{\partial x} = -\lambda_w\frac{\partial P_w}{\partial x} \end{aligned} \tag{10}$$

2.2.3.3 Combining Dary's law, mass balance and capillary pressure

The analytical equation for the counter current imbibition flow can be derived from the mass balance, darcy's law and capillary pressure described in section 2.2.3.1, 2.2.3.2 and 2.5 respectively.

$$\begin{aligned} u_t &= u_o + u_w \\ P_c &= P_o - P_w \end{aligned} \tag{11}$$

By rearranging the equations 10 and 11 one can obtain the following equation:

$$\begin{aligned} u_t &= -\lambda_w\frac{\partial P_w}{\partial x} - \lambda_o\frac{\partial P_o}{\partial x} \\ \lambda_w\frac{\partial P_w}{\partial x} &= -u_t - \lambda_o\left(\frac{\partial P_c}{\partial x} + \frac{\partial P_w}{\partial x}\right) \\ \lambda_w\frac{\partial P_w}{\partial x} + \lambda_o\frac{\partial P_w}{\partial x} &= \lambda_t\frac{\partial P_w}{\partial x} = -u_t - \lambda_o\left(\frac{\partial P_c}{\partial x}\right) \\ \frac{\partial P_w}{\partial x} &= -\frac{u_t}{\lambda_t} - \frac{\lambda_o}{\lambda_t}\frac{\partial P_c}{\partial x} \end{aligned} \tag{12}$$

In the case of the co current imbibition one can put equation 12 back into equation 10 which will result in the following equation

$$\begin{aligned} u_w &= -\lambda_w \cdot \left(-\frac{u_t}{\lambda_t} - \frac{\lambda_o}{\lambda_t} \frac{\partial P_c}{\partial x} \right) \\ u_w &= \lambda_w \frac{u_t}{\lambda_t} + \frac{\lambda_w \lambda_o}{\lambda_t} \frac{\partial P_c}{\partial x} \end{aligned} \tag{13}$$

2.2.3.3.1 Counter-Current imbibition equation In order to derive the counter current imbibition flow one has to look at the total fluid velocity. The total fluid rate is assumed to be zero due to the assumption that the oil and water has the same fluid rate, but with opposite directions. As u_t is set to zero and putting equation 13 going back into equation 10 the following equation is obtained.

$$u_w = \frac{\lambda_w \lambda_o}{\lambda_t} \frac{\partial P_c}{\partial x} \tag{14}$$

With the core in mind one can express the mass balance equation 7 as the water saturation change is equal to the amount of water that has moved into it.

$$\phi \frac{\partial S_w}{\partial t} = -\frac{\partial}{\partial x} \frac{\lambda_w \lambda_o}{\lambda_t} \frac{\partial P_c}{\partial x} \tag{15}$$

The capillary pressure is dependant on the water saturation and equation 15 can therefore be written as

$$\begin{gathered} \phi \frac{\partial S_w}{\partial t} = -\frac{\partial}{\partial x} \frac{\lambda_w \lambda_o}{\lambda_t} \frac{\partial P_c}{\partial S_w} \frac{\partial S_w}{\partial x} \\ \text{where} \\ \frac{\lambda_w \lambda_o}{\lambda_t} = \frac{\frac{Kk_{rw}}{\mu_w} \frac{Kk_{ro}}{\mu_o}}{\frac{Kk_ro}{\mu_o} + \frac{Kk_rw}{\mu_w}} = \frac{Kk_{ro}}{\mu_o} \cdot \frac{1}{1 + \frac{\frac{Kk_{ro}}{\mu_o}}{\frac{Kk_{rw}}{\mu_w}}} = \frac{Kk_{ro}}{\mu_o} \cdot \frac{1}{1 + \frac{k_{ro}}{k_{rw}} \frac{\mu_w}{\mu_o}} \end{gathered} \tag{16}$$

Equation 16 can finally be made into equation 1 by considering the fact that the change in oil saturation will be the same as the change in water saturation and by considering y and z directions.

$$\phi \frac{\partial S}{\partial t} = \frac{\partial}{\partial x} D(S_w) \frac{\partial S}{\partial x} + \frac{\partial}{\partial y} D(S_w) \frac{\partial S}{\partial y} + \frac{\partial}{\partial z} D(S_w) \frac{\partial S}{\partial z}$$

where

$$D(S_w) = -\frac{Kk_{ro}}{\mu_o} \cdot \frac{1}{1 + \frac{k_{ro}}{k_{rw}} \cdot \frac{\mu_w}{\mu_o}} \frac{dP_c}{dS_w}$$

2.2.3.3.2 Equation for Co-Current imbibition. Again putting equation 13 back into the mass balance equation 7 and consider the change in water saturation will give the equation

$$\phi \frac{\partial S_w}{\partial t} = -\frac{\partial}{\partial x}\left(\lambda_w \frac{u_t}{\lambda_t} + \frac{\lambda_w \lambda_o}{\lambda_t} \frac{\partial P_c}{\partial x}\right) \tag{17}$$

As can be seen by equation 17 it contains the total fluid velocity term which is cancelled out in the counter current flow equation. This is the main difference between the counter current and co current imbibition equations. This is possibly the reason for the co-current imbibitions faster recovery rate than the counter current rate as mentioned in section 2.2.1.

2.3 Wettability

As discussed in section 2.1 the wettability of a rock or matrix is important with regards to oil recovery in a fractured reservoir due to the fact that this will determine if spontaneous imbibition can occur or not. The wettability tells if the rock has a preference in contact with a certain liquid or gas over other liquids or gases. It is also a measurement of how much the solid prefers one fluid or gas over another. In the case of a reservoir the wetting phase will tend to spread out more on the rock surface (as can be seen in figure 6) and it will also have a tendency to imbibe into the porous media. This results in the expulsion of the non-wetting phases which is the whole concept of spontaneous imbibition.

In the case of oil and water in a reservoir there are three possible wettability scenarios. The porous media can be oil-wet, water-wet or neutral which will respectively make oil, water or both of the fluids adhere to the grains in the reservoir. If the angle between the water droplet, seen in figure 6, and the solid surface is less than 75 degrees the rock can be considered to be water wet [29]. If the angle is above 105 degrees it is considered oil wet, and any angle in between is seen as intermediately wet. The wettability is also an important factor due to the fact that it will determine the irreducible water saturation in the reservoir [29].

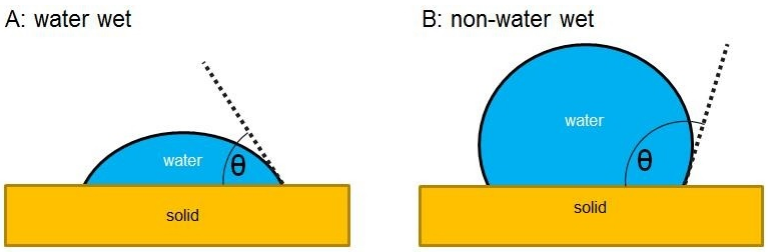

Source:[29]

Figure 6: *A: Display of how the wetting water face will tend to spread itself out on the surface of the media. B: Display of how the non-wetting face will tend to not spread itself out on the media.*

The wettability of a reservoir rock is an important factor when it comes to the mobility of the formation oil, and therefore oil recovery. If a reservoir is water-wet then the water will stick more to the reservoir grains and will let the oil flow easier through the reservoir towards the production well. If the reservoir is oil-wet then the oil will stick more to the reservoir grains and the water will flow easier towards the production well which will cause a faster water breakthrough and a higher residual oil saturation. Due to the reservoirs usually being heterogeneous [18] there can be different degrees of wettability at different parts of the reservoirs. The wettability of the reservoir matrix is also dependant on the saturation history of the rock such that parts of the reservoir that has been in contact with oil might be oil wet while parts that has not had any contact with oil might be water wet [1]. The wetting phase in one part of the reservoir can be the non-wetting phase in a different part of the same reservoir. This is important to take into consideration when looking at a reservoir core, as a core sample from one part of the reservoir could be oil-wet while a core plug from another part of the reservoir can be water-wet.

If a fractured reservoir is considered to be oil wet and spontaneous is impossible, then an alkaline or surfactant flooding might be considered to alter the wettability of the reservoir [19].

2.3.1 Determination of wettability

There are many different methods to determine the wettability of a reservoir.

One method to determine the wettability of a reservoir is called the contact angle method.

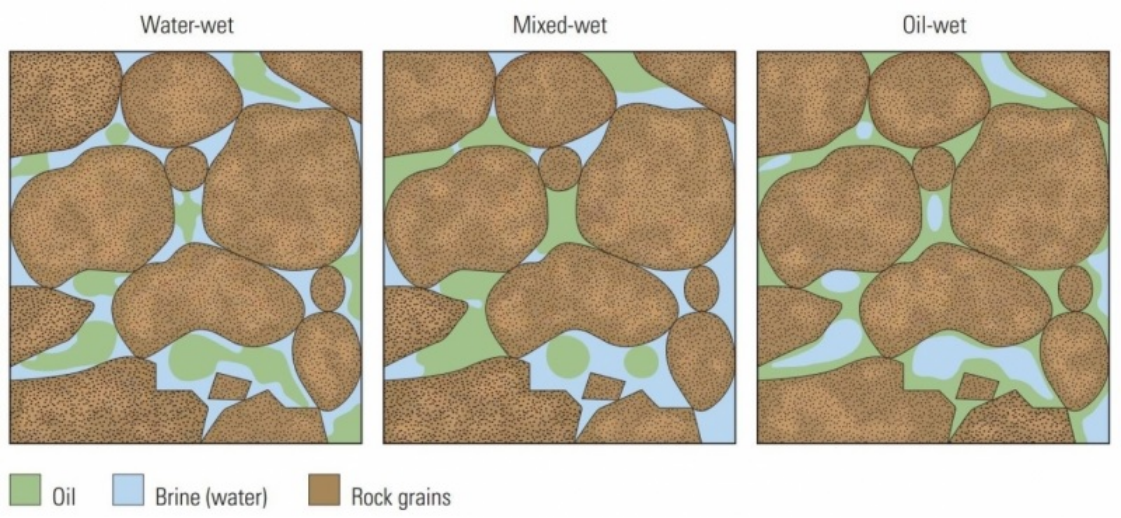

Source:[29]

Figure 7: *Shows how the oil and water can stick to the reservoir grains in a water wet, mixed wet and oil wet reservoir rock going from left to right respectively.*

This method use a core sample and use a microscope to observe how a drop of oil or water will shape itself when dropped on the core surface. This is one of the most accurate methods to determine the wettability for artificial cores materials and pure liquids [11]. This method can be highly inaccurate however for porous media using reservoir fluids. This is due to a number of different reasons such as alterations to the core due to poor handling of the core, or alterations caused by the use of certain drilling fluids. Another reason is that in order to get a good measurement of the contact angle the surface has to be smooth and one can therefore not measure the angle directly on a core [1].

Another method uses the information gathered from the affect the wettability has on the relative permeabilities. Usually in an oil wet reservoir the residual oil will be a bit higher than for other cases and the irreducable water saturations will usually be a bit lower. This is due to oil having a more restricted movement as it will tend to stick to the rock while the water will flow more freely. In the case of a water wet rock the opposite is true as the irreducable water saturation is usually higher and the residual oil saturation tends to be lower. Another characteristic for the relative permeabilities in an oil wet system is that the crossing point between the oil and water relative permeability curves lies more towards the middle of the plot making a symmetrical plot which can be seen figure 8. In a water wet

rock the crossing point between the relative permeability curves lies more towards the right side of the plot, towards the 100% water saturation point as can be seen in the right plot in figure 8.

In the case of a strongly water wet system the relative permeability of oil will be relatively high at the irreducible water saturation. This is because the water is located in small pores and has little effect on the flow of oil. On the other end the effective water permeability is relatively low at the residual oil saturation due to some of the oil being trapped as spheres in the center of the large pores. Therefore the water permeability at S_{or} is much lower than the oil permeability at S_{iw}. In the case of a strongly oil wet system the opposite is true for the relative permeabilities [4].

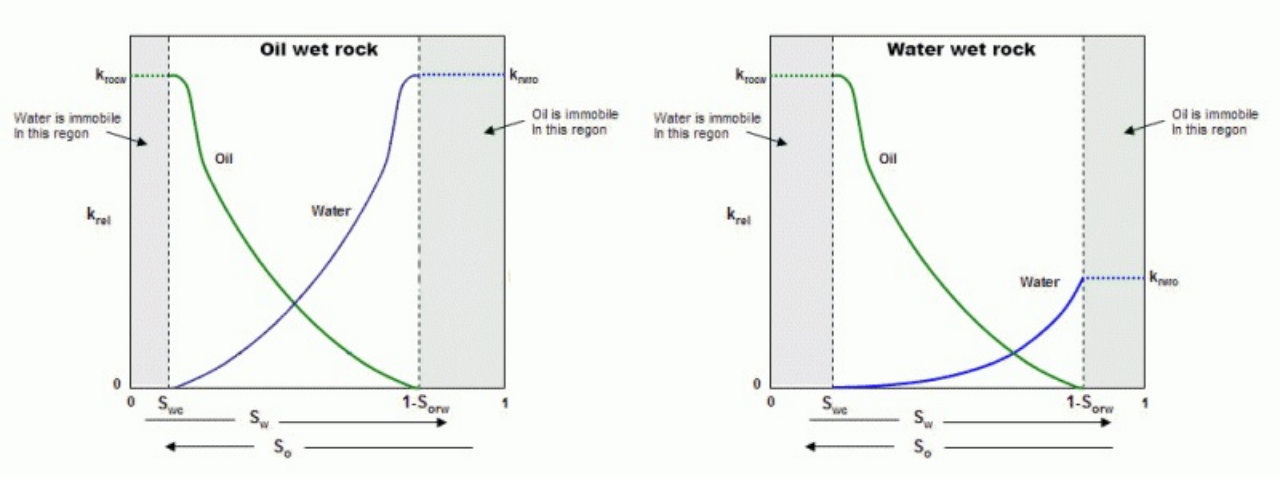

Source:[29]

Figure 8: *Left figure shows how the relative permeability curves for water and oil typically will look like in a oil wet rock. Right figure shows how the relative permeability curves for water and oil typically will look like in a oil wet rock.*

Another way to measure the wettability is to measure the characteristics of a core plugg in an Amott imbibition test or a USBM test [22].

2.3.1.1 Amott test

In an Amott test the wettability of a porous medium is measured as a function of the displacement properties of the rock-water-oil system. The Amott-Harvey tests consists of a

Source:[23]

Figure 9: *An ambient temperature Amott cell setup to measure spontaneous imbibition.*

process of four steps which includes [2]

1. A sample at irreducable water is placed into a water filled tube (distilled water in the case for the tests discussed in this thesis). The sample is then left in the tube over a period of time which usually lasts for at least 10 days. This will trigger the spontaneous imbibition process described in section 2.2. This will give final water saturation after the spontaneous imbibition noted as S_{ws}.

2. The core is then placed in a flow cell and flooded with water in order to reduce the oil saturation down to residual oil saturation, S_{wor}, and the additional oil recovery is noted.

3. The core is now at S_{wor} and process from step 1 is repeated with a tube filled with oil instead of water. This gives spontaneous uptake of oil up to a certain saturation, which in turn gives a new water saturation, S_{wos}.

4. The core is now placed in a flood tube again where oil is forced through the core which

further reduces the water saturation to the residual water saturation, S_{wr}.

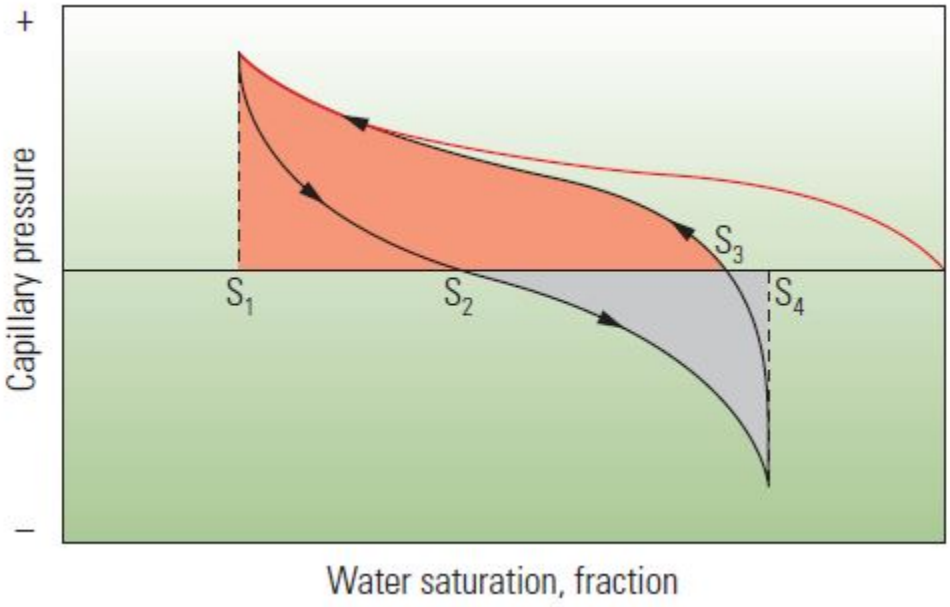

Source:[1]

Figure 10: *A picture showing the Amott-Harvey test process in relation to the capillary pressure on the y-axis versus the water saturation on the x-axis. The red area has positive capillary pressure while the grey area has negative capillary pressure. The process starts of with step 1 at $S_1 = S_{wi}$ and follows the lower curve with the arrow to $S_2 = S_{ws}$. Step 2 starts at S_2 and again follows the arrow down and ends at $S_4 = S_{wor}$. Step 3 starts at the lowest point on the capillary pressure axis at saturation S_4 and ends up at $S_3 = S_{wos}$. The last step 4 then goes from S_3 and follows the arrow up to the highest point on the capillary axis and reach S_{wr}.*

This four step process is used in order to calculate the ratios of spontaneous imbibition for oil, I_o, and water, I_w.

The following formulas are used to calculate the ratios of spontaneous imbibition for water and oil, and the Amott-Harvey index respectively.

$$I_w = \frac{S_{ws} - S_{wi}}{S_{wor} - S_{wi}} \tag{18}$$

$$I_o = \frac{S_{wor} - S_{wos}}{S_{wor} - S_{wr}} \tag{19}$$

$$I_{A-H} = I_w - I_o \tag{20}$$

The Amott-Harvey index, I_{A-H}, is the difference between the water index and the oil index and will give a number between +1 and -1, where +1 indicates a strongly water wet core and -1 indicates a strongly oil wet core [1].

2.4 Relative permeability

Permeability is the ability that a porous media has to let fluids pass through it and it depends on both size, length and amount of interconnecting pores [32]. The absolute permeability is the permeability when a porous medium is 100% saturated with a single fluid [25].

The relative permeability is a concept that uses the absolute permeability of a porous medium and the effective permeability of a fluid when the fluid only occupies a fraction of the overall pore volume. The relative permeability depends on multiple factors such as pore geometry, wettability, fluid distribution and the fluid saturation history. Measurements of the relative permeability can be done on core samples in a laboratory, but such tests are both expensive and takes a considerable amount of time [26]. Relative permeability is a very important characteristic of the reservoir due to the fact that there will almost always be multiphase flow with water, oil and/or gas.

There exist multiple models to calculate and compare the relative permeabilities with other reservoir properties, such as Brooks-Corey, Carman-Kozeny models, Chierici model and many more. In this thesis the Brooks-Corey power law is used to calculate the relative water and oil permeability for different water saturations in the core [27].

$$\begin{aligned} k_{rw} &= k_{rw,max}\left(\frac{S_w - S_{wc}}{1 - S_{or} - S_{wc} - S_{gc}}\right)^{n_w} \\ k_{ro} &= k_{ro,max}\left(\frac{S_o - S_{or}}{1 - S_{or} - S_{wc} - S_{gc}}\right)^{n_o} \\ k_{rg} &= k_{rg,max}\left(\frac{S_g - S_{gc}}{1 - S_{or} - S_{wc} - S_{gc}}\right)^{n_g} \end{aligned}$$

In this thesis and the experiments described in section 3 there are no gas present in the

cores or the simulation models. The above equations can therefore be reduced from three equations to two equations where the gas term can be neglected:

$$k_{rw} = k_{rw,max}\left(\frac{S_w - S_{wc}}{1 - S_{or} - S_{wc}}\right)^{n_w} \tag{21}$$

$$k_{ro} = k_{ro,max}\left(\frac{S_o - S_{or}}{1 - S_{or} - S_{wc}}\right)^{n_o} \tag{22}$$

One important note is that the corey exponents n_o and n_w has a range of 1 - 6 [27].

2.5 Capillary pressure

As mentioned in section 2.2 the capillary pressure is considered to be the main driving mechanism for spontaneous imbibition. The capillary pressure is the pressure difference that exists over the interface between two phases or fluids due to capillary forces [3]. The capillary forces are surface tension and interfacial tension, where the surface tension is the tension that exists in the interface between a liquid and gas while interfacial tension is the tension that exist on the interface between two immiscible fluids.

In a porous media the capillary pressure is defined as the pressure difference between the pressure in the non-wetting phase and the pressure in the wetting phase.

There exists many different formulas for the capillary pressure that is used in different scenarios. In a scenario where a drop of water exists in a volume of oil (as can be seen in figure 11) the capillary pressure is defined as [30]

$$P_c = P_0 - P_w = \frac{2\sigma}{r} \tag{23}$$

In the case of a water wet surface where a water drop is surrounded by the surface and oil the equation becomes [6]

$$P_c = P_o - P_w = \frac{2\sigma\cos\theta}{r} \tag{24}$$

Because a porous media is a complex system it is often idealized by imagining a large number of small capillary tubes. This way the capillary pressure can be expressed similarly to equation 23 that is designed for a perfect spherical drop.

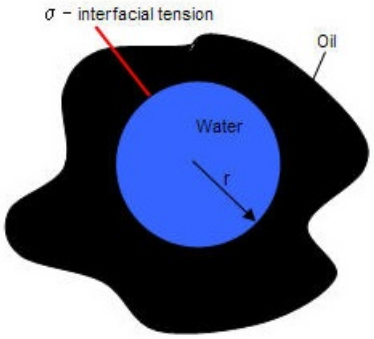

Source:[30]

Figure 11: *A figure showing a spherical drop of water inside a volume of oil.*

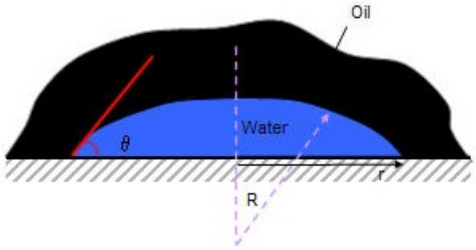

Source:[30]

Figure 12: *A figure showing how water will spread out on a water-wet surface when there are both water and oil at the surface area.*

As illustrated in figure 13 a capillary tube where the interface between the water and oil stands still, the interfacial tension that is dragging the water to the right has to be equal to the pressure forces that is pushing towards the left.

$$\begin{aligned} \frac{P_o - P_w}{A_c} &= 2\pi r_c \sigma \cos\theta \cdot \\ P_o - P_w &= \frac{2\sigma\cos\theta}{r_c} \end{aligned} \tag{25}$$

In the permeability section 2.4 it was mentioned that the Brooks-Corey power law was used to generate relative permeability tables for different degrees of water saturations. In order to get a simulation running there is a need for a capillary pressure that corresponds to each of the saturations that are given in the relative permeability curves as well. Therefore a capillary pressure equation that is dependent on saturations has to be used. One such

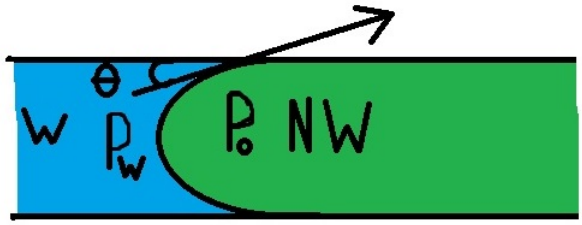

Figure 13: *A drawn figure of how the wetting phase (water) will try to drag itself (due to interfacial tension) on the edges of a capillary tube while the non-wetting phase (oil) is pushed to the left in the middle of the tube due to capillary pressure.*

equation is a slightly altered version of Brooks and Corey's power-law equation for primary drainage [14]

$$P_c = \frac{c_w}{\left(\frac{S_w - S_cw}{1 - S_cw}\right)^{a_w}} \tag{26}$$

Equation 26 is valid for a completely water-wet core, while it can also be used for a completely oil-wet core by changing the water saturations with the corresponding oil saturations. In order to get an equation that would be valid for cores that are not 100% water or oil wet a new equation was developed by Skjaeveland. They did so by looking at equation 26 and adding the water-wet version and the oil-wet version together which would give a symmetrical form that should be correct for both the extreme cases [14].

$$P_c = \frac{c_w}{\left(\frac{S_w - S_{cw}}{1 - S_{cw}}\right)^{a_w}} + \frac{c_o}{\left(\frac{S_o - S_{or}}{1 - S_{or}}\right)^{a_o}} \tag{27}$$

In equation 27 the a's and c's are constants where there are one set for imbibition and one set for drainage. The constraints that has to be followed when choosing these constants is that a_w, a_o and c_w are positive numbers while c_o is a negative number. In this thesis it was chosen to use equation 27 as this is considered to be more accurate for a core that is water-wet, but not 100% water-wet.

2.6 Diffusion process

A diffusion process can be describes as a process where a substance (such as a fluid or gas) moves from a position of high concentration to a position of a lower concentration. An example of this is the oil in the core with a high concentration of oil that migrates out into the water, with lower concentration of oil, surrounding the core. This process can often be described by a diffusion equation that can is generally non-linear. The equation derived in section 2.2.3.3 is an example of a diffusion equation that describes the change of saturation of oil over time in the core. This diffusion equation is generally a partial non-linear differential equation.

2.6.1 Linear diffusion

Linear diffusion is when the process can be expressed with an equation where the D is not dependant on the term that the equation itself are describing [16]. Equation 2.2.3.3 is a linear diffusion equation as long as D is not dependant on the saturation. The linear diffusion equation can then be expressed as

$$\frac{\partial S}{\partial t} = D\frac{\partial S}{\partial^2 x} + D\frac{\partial S}{\partial^2 y} + D\frac{\partial S}{\partial^2 z} \tag{28}$$

where the D is constant. This is a much simpler equation to solve than an equation where the diffusion term D is dependant on the saturation of the core. Due to the complexity of the non-linear equation it is of interest to see if the diffusion equation given in equation 2.2.3.3 can be described as a linear diffusion equation.

2.6.2 Non-linear diffusion

A non-linear diffusion equation is an equation where the diffusion term D is dependant on the change of another term [16]. In this thesis the D is dependant on saturation which makes it complicated due to the fact that the equation itself is supposed to be solved to see change in saturation.

The equation derived in section 2.2.3.3 has a diffusion term D that is dependant on the saturation and is generally a non-linear equation. This a much harder equation to solve and

in this thesis it will, by the use of simulations, be attempted to see if the diffusion term D can be held constant and give the same results in terms of change of the core saturations over time.

If equation is non-linear then the equation can will be expressed as

$$\frac{\partial S}{\partial t} = \frac{\partial}{\partial x} D(S_w) \frac{\partial S}{\partial x} + \frac{\partial}{\partial y} D(S_w) \frac{\partial S}{\partial y} + \frac{\partial}{\partial z} D(S_w) \frac{\partial S}{\partial z} \tag{29}$$

2.7 Numerical and analytical solutions

There are two main ways to solve equations. One is the numerical route and the other is the analytical route. In general the analytical route is the most accurate method, but sometimes an equation is hard or even impossible to solve analytically and therefore a numerical approach is needed.

2.7.1 Numerical solution

A numerical approach is an approach that uses numerical approximations. One approach is to make a number of guesses or iterations to find the correct solution [7]. An example of this is for an equation $x^2 - 4 = 0$ and make a guess that $x = 3$ which results in $3^2 - 4 = 5$. Then another guess can be made for example $x = 1 \rightarrow 1^2 - 3 = -2$. As one guess gave a negative number and the other gave a positive number one can conclude that the right answer lies between $x = 1$ and $x = 3$.

Another example of using a numerical approach to find an estimation of complex functions is the use of the trapezoidal rule to find an approximation of the area under a graph or a curve [24]. This approach has been used in this thesis in order to find an approximation of the total area under the diffusion coefficient curve. It states that the area under the curve can be estimated by creating a series of trapezes under the curve with a set interval on the x axis. The equations becomes

$$\begin{gathered} A_i \approx \frac{\Delta x}{2} \left(f(x_{i-1}) + f(x_i) \right) \\ \int_a^b f(x) \approx \frac{\Delta x}{2} \left(f(x_0) + f(x_1) \right) + \frac{\Delta x}{2} \left(f(x_1) + f(x_2) \right) + ... + \frac{\Delta x}{2} \left(f(x_{n-1}) + f(x_n) \right) \end{gathered} \tag{30}$$

These estimation of the area under a curve is a decent approximation when the integral becomes to difficult to solve and the smaller the Δx interval is the more accurate the approximation becomes. An example of how this method looks on a curve is given in figure 14.

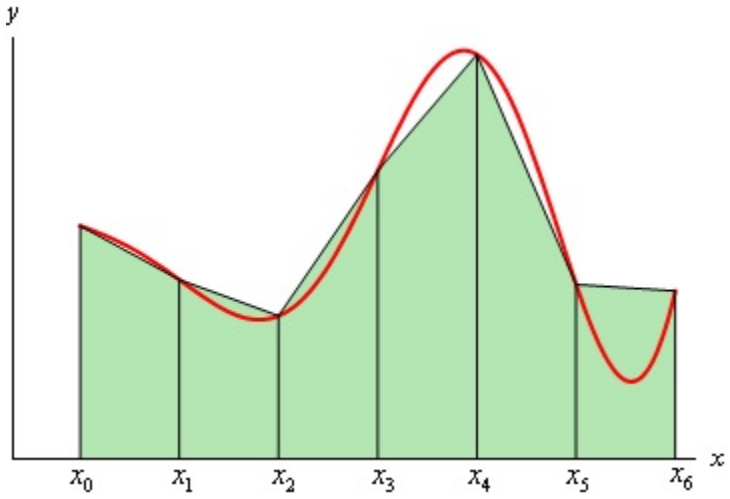

Figure 14: *An example of how it looks like when estimating the area under a curve with the use of the trapezoid method.*

When there is a derivative such as the capillary pressure in the diffusion equation 2 one can express this numerically.

The definition of a derivative is [28]

$$\begin{aligned} \frac{df(x)}{dx} &= \lim_{x \to a} \frac{f(x) - f(a)}{x - a} \\ &\lim_{h \to 0} \frac{f(a+h) - f(a)}{h} \\ &\lim_{\Delta x \to 0} \frac{f(x + \Delta x) - f(x)}{\Delta x} \end{aligned} \tag{31}$$

and this can then be used to express an approximation of the derivative by changing it up to

$$\frac{df(x)}{dx} \approx \frac{f(x_1 + \Delta x) - f(x_1)}{(x_1 + \Delta x) - x_1} = \frac{f(x_2) - f(x_1)}{x_2 - x_1} \tag{32}$$

2.7.2 Analytical solution

The analytical solutions gives an exact solution to the mathematical problem that is of question. In the problem $x^2 - 4 = 0$ the analytical and exact solution can easily be solved to be $x^2 = 4 \rightarrow x = \sqrt{4} = 2$ [7]. The more complex the equation is and the more variables that it depends on the harder it is to be solved analytically. The diffusion coefficient in equation 29 is generally dependant on the water saturation which makes the whole diffusion equation much harder to solve analytically due to it being a non-linear equation.

2.8 Eclipse

Eclipse is a simulation program that uses numerical algorithms in order to solve and predict an outcome for its given input data. Eclipse requires a lot of different input data in order to run. Some of the main reservoir characteristics that is required are the relative permeability curves and their corresponding capillary pressure, the porosity and the permeabilities. The model also needs a grid that gives the size and structure of the model.

The eclipse model used in this thesis is supposed to represent an oil filled core that is surrounded by water. The model consists of a radial grid of $40 \times 20 \times 40$ as can be seen in figure 15.

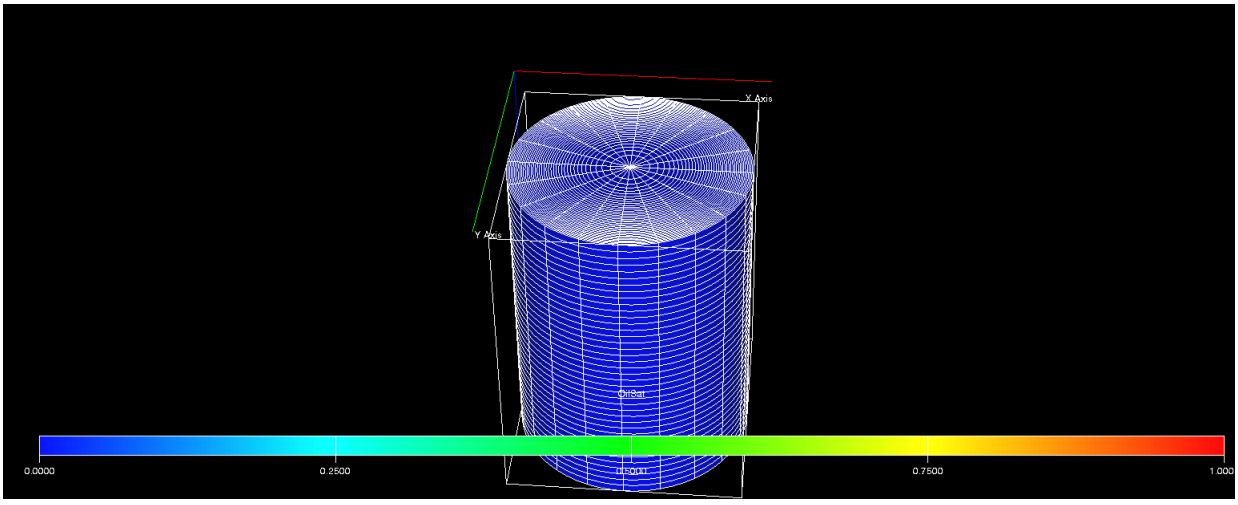

Figure 15: *A picture of the whole grid that is used in the simulator. The outer parts contains 100% water in the initial stage while a core of 100% oil is inside.*

As can be seen in figure 15 the model is a cylinder of water that represents the water surrounding the core. Inside this cylinder of water there is a $20 \times 20 \times 20$ reservoir core filled with oil as can be seen in figure 16.

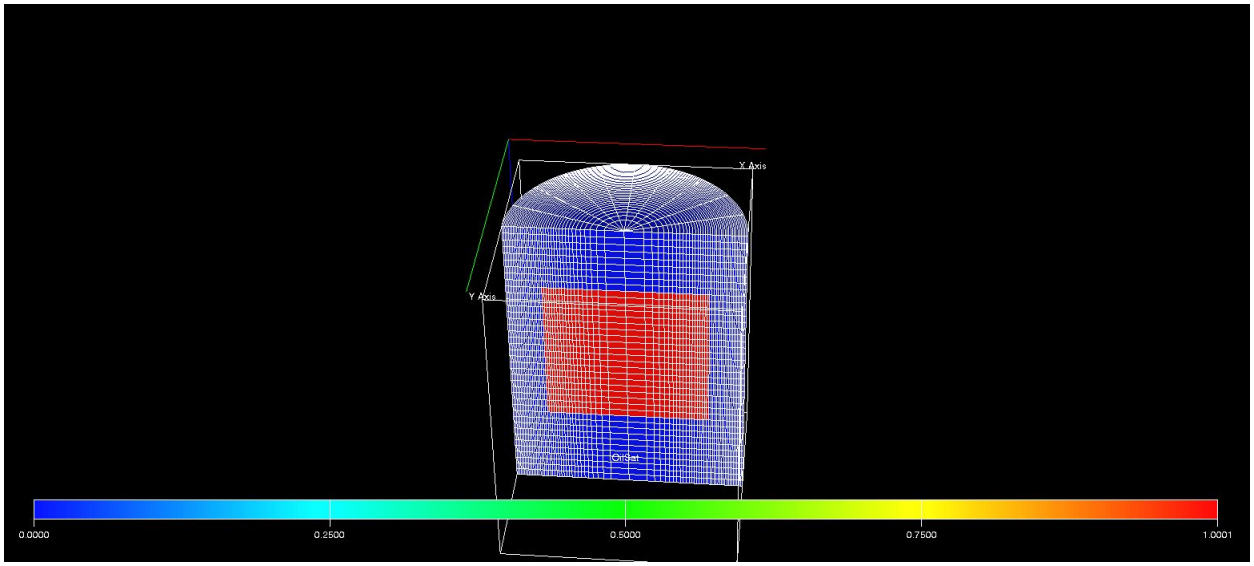

Figure 16: *Half of the simulation model at timestep 0 where all of the oil is still in the core and the water surrounding it.*

The core plug has a much lower porosity, permeability and fluid volume than the rest of the model. This is in order to make a best possible representation of the imbibition process that takes place during the tests conducted by Standnes [15]. There is also placed a no flow boundary on the top and bottom of the red core in figure 16. This is due to the cores being coated on the top and bottom in the experiments as discussed in the next section 3.

The relative permeability and capillary pressures used in the model are calculated with formulas described in section 2.4 and 2.5.

The time steps that are used are relatively small and goes by increments of 0.001 hours for the first 500 steps, and increases up to 0.2 hours for the last 500 steps.

3 Background tests

In the imbibition tests conducted by Dag Chun Standnes the oil phase used was n-Decane from Riedel-deHäen with grade above 95%. This oil has no polar components and will therefore not change the wettability of the cores. The imbibing water phase used was distilled water.

The porous medium used were outcrop chalk samples from Denmark where the samples were taken from the same block and the porosities were close to 42%, and the absolute permeabilities were determined to be approximately 2 mD. Both the top and bottom faces of the cylindrical cores were coated with Glasfiberspackel (polyester) from Hagmans Kemi AB Sweden in order to get no flow boundaries on the top and bottom surface areas of the core. The no flow boundaries on the core restricts the water and oil movements to the sides of the core and reduces the impact of the gravity force on the imbibition process. Due to the restricted effect of gravity it is neglected in this thesis.

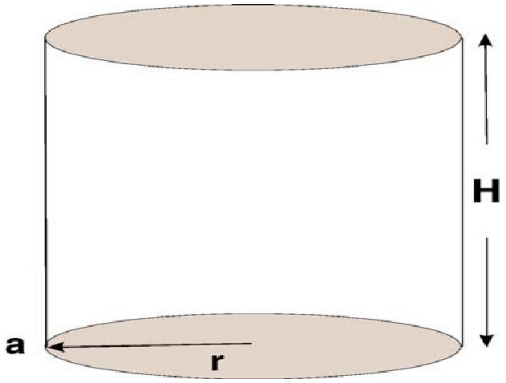

Source:[15]

Figure 17: *Here the upper and lower surface areas are darker to illustrate the fact that they are coated and no flow boundaries. H represents the height of the core and a represents the radius.*

All of the tests were performed at about 20°C, and were performed with the use of Amott cells with the exception of the two cores that had a diameter of 6.00 and 10.00 cm. For the two cores with diameters 6.00 and 10.00 cm the samples were suspended from a balance and immersed in distilled water. All of the cores were 100% oil saturated which means that there were no connate water in the beginning of the tests. The cores were placed inside the

Amott cells, which was then filled with distilled water and the oil production was measured as a function of time. The change in weight of the cores were measured and the mass of the samples was determined after each run to check the material balance and if there was a good match between measured volume of water imbibed and the weight of the rock sample from the tests [15].

$$\phi\frac{\partial S}{\partial t} = \frac{\partial}{\partial x}D(S_w)\frac{\partial S}{\partial x} + \frac{\partial}{\partial y}D(S_w)\frac{\partial S}{\partial y} + \frac{\partial}{\partial z}D(S_w)\frac{\partial S}{\partial z} \tag{33}$$

where

$$D(S_w) = -\frac{kk_{ro}}{\mu_o}\cdot\frac{1}{1+\frac{k_{ro}}{k_{rw}}\cdot\frac{\mu_w}{\mu_o}}\cdot\frac{dP_c}{dS_w} \tag{34}$$

The unit of $D(S_w)$ is m^2/s and is called the capillary diffusivity coefficient (CDC). k is absolute permeability (m^2), k_{ro} is relative permeability of oil, k_{rw} is relative permeability of water, μ_o is the oil viscosity (Pas), μ_w is the water viscosity (Pas), P_c is the capillary pressure (Pa), S_w is the normalized water saturation (m^3/m^3), t is the imbibition time (s) and ϕ is the fractional porosity (m^3/m^3).
With the use of radial coordinates due to the cylindrical shape the formula turns to:

$$\frac{\partial^2 S}{\partial r^2} + \frac{1}{r}\cdot\frac{\partial S}{\partial r} = \frac{\phi}{D}\cdot\frac{\partial S}{\partial t} = \frac{1}{\alpha^2}\cdot\frac{\partial S}{\partial t} \tag{35}$$

where, $\alpha^2 = \frac{D}{\phi}$ (m^2/s) is assumed to be constant and independent of S_w.

The diffusion coefficient D is generally dependant on water which, as mentioned before, makes the counter current imbibition equation difficult to solve analytically.

4 Results and discussion

In order to get a understanding on how the diffusion coefficient works and how it affects the oil recovery, it is attempted in this thesis to create a simulation that gives realistic results based on the test that was performed by Standnes in 2004 [15]. It is therefore important to get a good history match between the experiment and the simulation in order to have a simulation that gives valid responses. It is however also important to know that one match between the simulator and the experiments does not equal that there is a unique solution. In other words although one can create a match between the simulation and the experiments this does note necessarily mean that the input data are correct as one can have more than one set of input data which will create a good match.

A base case of a simulator was given by Dag Standnes along with his paper with the information about the experimental tests that are referred to in this thesis [15]. Some relative permeability curves and capillary pressure curve from a previous bachelor student, Markus Moe, [10] was also given.

The base case of the simulator given by Dag Chun Standnes was ran for all four core cases of different diameter cores to see how much difference there was between the observed laboratory results and the general simulation. When running these initial simulations for the different cores, the grid had to be changed due to the size differences, along with the porosity and residual oil saturation as can be seen in table 1. The permeability was set as constant of for all four cores at 2 mD as this is what is given from the paper [15].

Core size/Paramterers:	$S_{or}(\%)$	Height (cm)	$\phi(\%)$
1.99 cm Diameter core	41.6	5	43.0
3.39 cm Diameter core	39.8	4.96	42.6
6 cm Diameter core	31.1	3.2	42.4
10 cm Diameter core	32.3	3.97	43.2

Table 1: *Some of the different parameters that has to be considered when constructing the grid and model for the different core cases.*

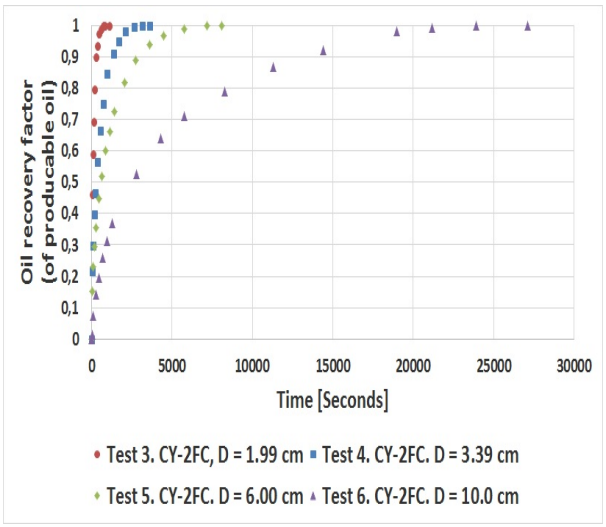

(a) *The test results from paper [15] with time in seconds and normal scale on the x axis and oil recovery on the y-axis.*

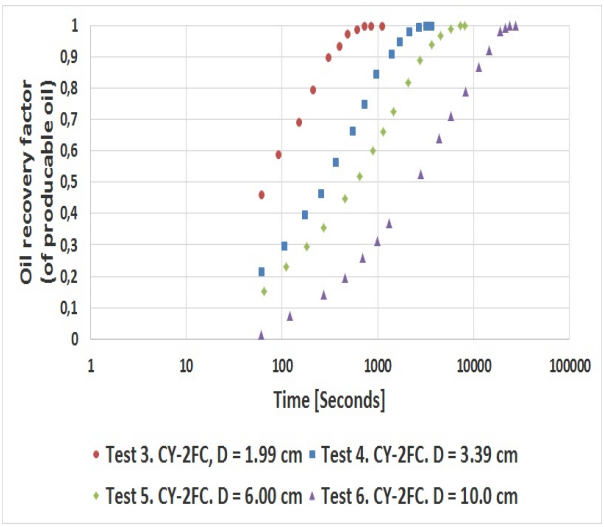

(b) *The test results from paper [15] with time in seconds and logarithmic scale on the x axis and oil recovery on the y-axis.*

Figure 18: *A figure showing the oil recovery that was observed by Dag Chun Standnes in the tests described in section 3. All four tests had closed faces on the top and bottom of the core as illustrated in figure 17. The cores in test 3, 4, 5 and 6 had a diameter of 1.99 cm, 3.39 cm, 6.00 cm and 10.0 cm respectively.*

The base cases gave a production curve that was far of from the experimental data and it was therefore decided to try out Moes relative permeabilities and capillary pressure to see how these would compare to both the experimental data and the initial base case. The results for both the initial base case, the run with Moes input data and the experimental data can be seen in figure 19 for all four cores.

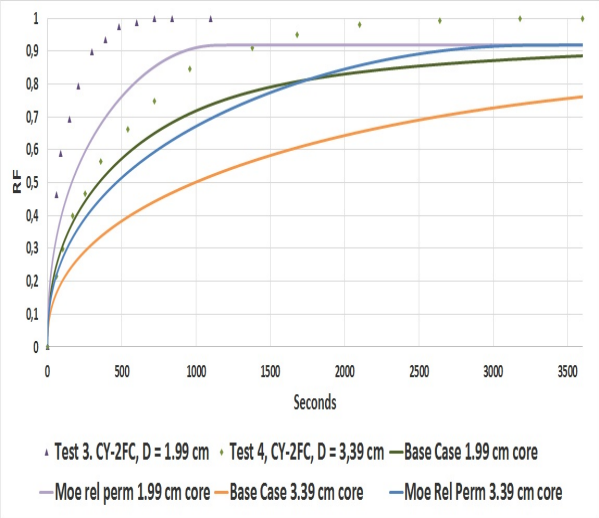

(a) *Results from the simulation for the core sizes 1.99 cm from test 3 and 3.39 cm from test 4. Both for base case and Moes permeabilities and capillary pressure.*

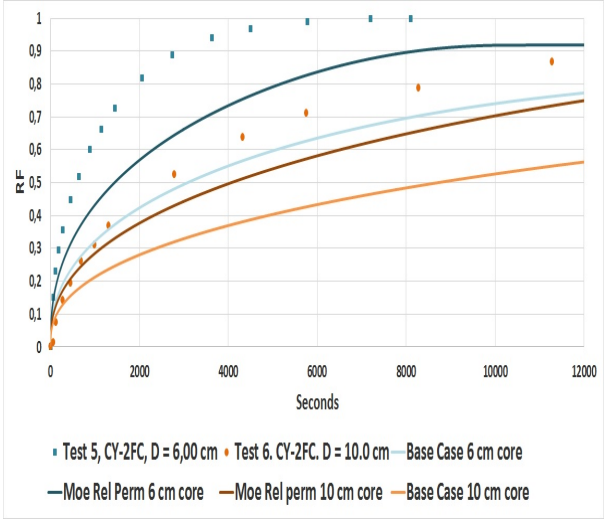

(b) *Results from the simulation for the core sizes 6.00 cm from test 5 and 10.0 cm from test 6. Both for base case and Moes permeabilities and capillary pressure*

Figure 19: *This figure shows the difference between the oil recovery observed in the different core experiments and the initial simulations of the oil recovery both for the initial base case and the base case modified for Moe's relative permeabilities and capillary pressure.*

As can be seen in figure 19 both the initial base case and the case with Moes data are quite different from the experimental data. Moes data was however significantly closer to the experimental curve than the initial base case and it was therefore decided to find the parameters that would give the same relative permeabilities and capillary pressures that Moe had used. These parameters where found by plotting relative permeabilities and capillary pressures from Moes bachelor thesis along with another set of relative permeabilities and capillary pressure that were calculated in excel. The calculated relative permeabilities and capillary pressure was created using equations 21, 22 and 27. These equations are dependant on the variables nw, no, $krw*$, $kro*$, cw, aw, co and ao and these parameters were adjusted until the three different graphs gave a relatively close match.

4.1 Finding Relative permeability curves

When finding the input data nw, no, $krw*$, $kro*$ that would give the closest possible match with the relative permeabilities from Moes bachelor thesis, it was decided create another table which gave the difference between the relative permeabilities from Moes bachelor thesis and the relative permeabilities created by own input data. This table was then summed up to give a number for the total difference between the graphs and the input data was then varied in order to minimize this number. With the use of the equations described in section 2.4 a set of different values for No, Nw, $krw*$ and $kro*$ was found to get a close match between the relative permeability curves created from the functions and the data from Moe's thesis [10]. This resulted in the relative permeabilities in table 12.

Table 12 is a relatively close match with the table from Moes bachelor thesis which can be seen and demonstrated in figure 20 where the calculated curves and the curves from Moes data are plotted together.

The data used to get table 12 is shown in table 2.

nw	**no**	**krw***	**kro***	**cw**	**aw**	**co**	**ao**
3	1.19	0.199	1	0.7	0.65	-0.06	1

Table 2: *Values for the different parameters used to create table 3*

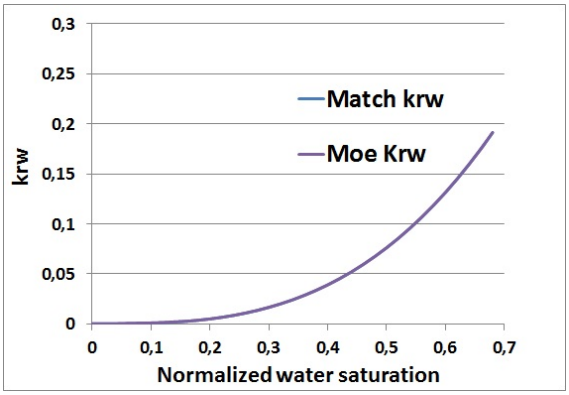

(a) Plot of Moes relative water permeability curve and the calculated curve to match it.

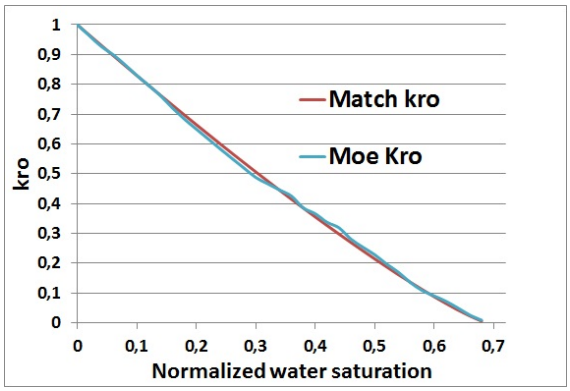

(b) Plot of Moes relative oil permeability curve and the calculated curve to match it.

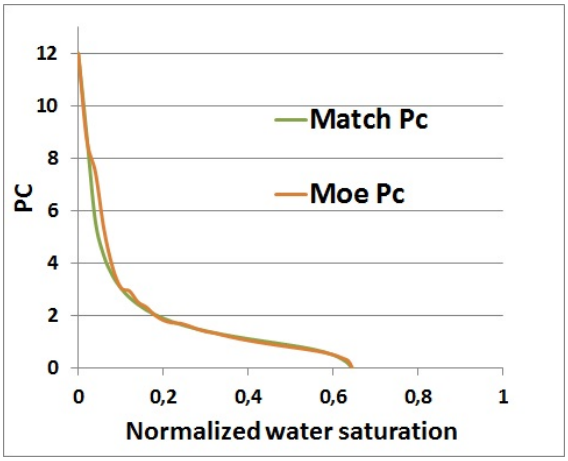

(c) Plot of Moe's capillary pressure curve and the calculated curve to match it.

Figure 20: *Figure demonstrating the difference between the calculated data that has been used as a starting point and the data provided from Moes thesis.*

4.2 Sensitivity tests for capillary pressure curve

Due to the relationship between the diffusion equation and the capillary pressure curve it follows that when the capillary pressure curve is changed the values of D at different saturations will change. From equation 2 it follows that the diffusion equation is dependant on both the relative permeabilities and the change in capillary pressure (which again is dependant on water saturation). From the equation it can also be seen that if the relative permeabilities are kept constant the relationship between the diffusion coefficient and the derivative of the capillary pressure becomes a linear equation dependant on the derivative of the capillary pressure, with respect to water saturation. It was therefore decided to continue with the same relative permeabilities found in section 4.1 and manipulate the capillary pressure curve to get a good history match as this would give a more easily monitored change in the diffusion coefficient than changing the relative permeabilities.

As can be seen in figure 19 the data from Moes bachelor thesis gave a closer match than the base case for all four tests, and it was therefore decided to use the capillary pressure curve from section 4.1 as the starting point for the history match. As the Skjaeveland capillary pressure curve is affected by four different parameters as seen in section 2.5 it is important to have an understanding of how each parameter affects the capillary pressure curve and how this again affects the recovery factor versus time. A short sensitivity was done in order to see how each parameter affected the capillary pressure curve and how it also affected the recovery factor in the simulations. The results can be seen in figure 21 and 22.

From figure 21a it can be seen that an increase in the term *cw* gives an increase in the capillary pressure curve for the whole water saturation interval, although it looks like it contributes to a higher increase in value for the water saturation from 0 to 50% and a smaller increase for water saturations above 50%. Figure 21a also indicates that increasing aw gives a relatively large increase for water saturations up to 50% while it barely increases the capillary pressure towards the end of the saturation interval. From the same figure it can be observed that an increase in the *co* value gives an increase in capillary pressure for the later parts of the water saturations while the beginning parts seems to stay the same. The opposite can be said about changing the *ao* as an increase in this value gives a lower

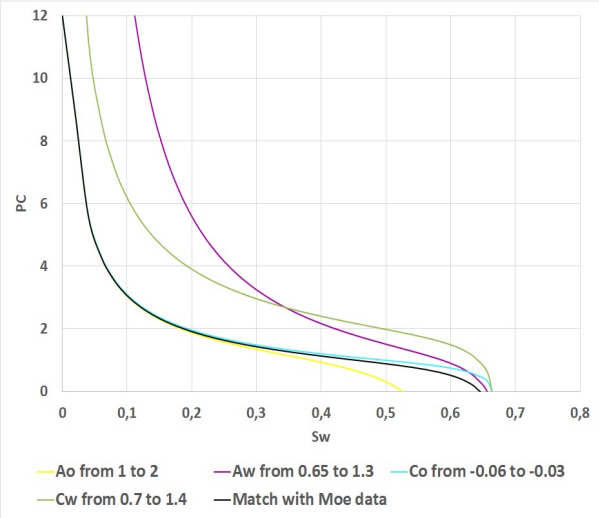

(a) *Figure showing how the capillary pressure curve is affected by increasing one of the following parameters cw, aw, co and ao. One parameter is changed at the time while the others are kept constant and kept the same as in table 2.*

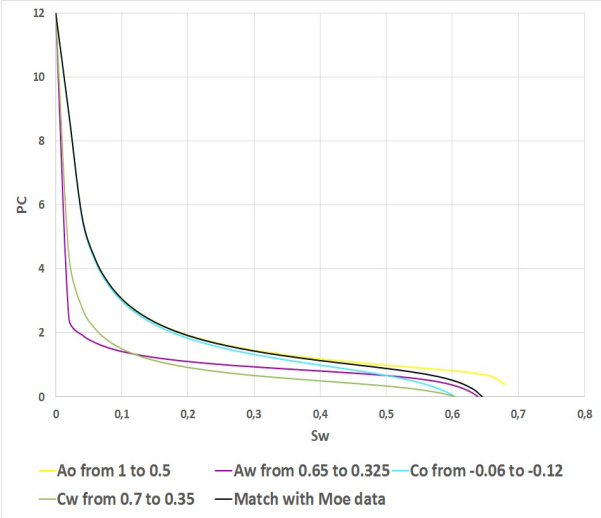

(b) *Figure showing how the capillary pressure curve is affected by decreasing one of the following parameters cw, aw, co and ao. One parameter is changed at the time while the others are kept constant and kept the same as in table 2.*

Figure 21

capillary pressure on the later parts of the saturation interval and it gives an earlier crossing point between the capillary pressure and the water saturation axis.

From figure 21a it can be seen that a doubling of each individual input data gives an increase in capillary pressure and a later crossing point for all input parameters except for *ao* which gives an earlier crossing point and a lower capillary pressure towards the end.

The exact opposite can be observed in figure 21b where again the *aw* and *cw* input parameters seems to have the biggest impact on the whole curve and especially on the beginning water saturations. All parameters here except for *ao* gives a reduced capillary pressure curve and earlier crossing point while the reduction of *ao* gives a higher capillary pressure curve towards the end and a later crossing point.

From figure 22a it can be seen that cutting the *co* value in half results in a slower, but similar shape of production curve as the initial case and it has a lower production plateau for the given time period. Cutting the *cw* in half however gives a relatively different shape of production curve and has a slower production rate, but has the same production plateau

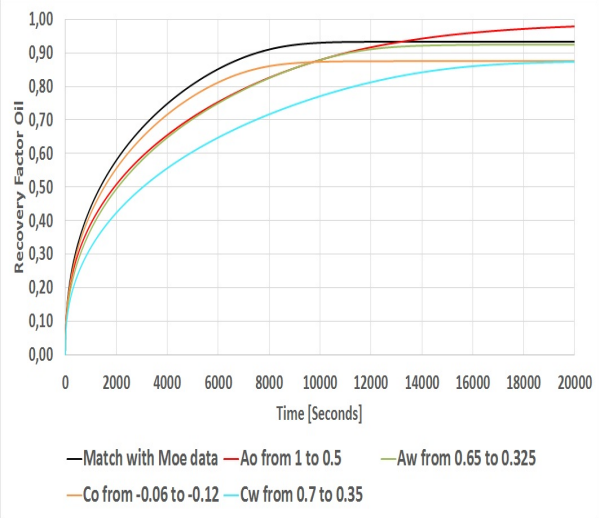

(a) *A figure showing how the production rate changes as the different relative permeability input data are (one at a time) cute in half.*

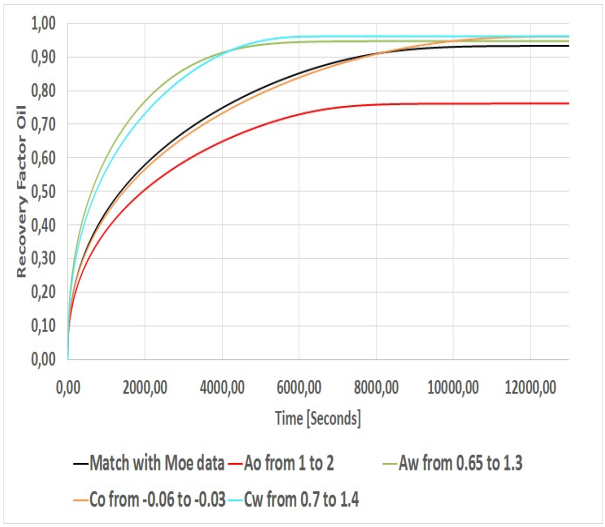

(b) *A figure showing how the production rate changes as the different relative permeability input data are (one at a time) doubled.*

Figure 22

for this time interval. Cutting the *ao* and *aw* in half gives quite similar results to each other although the new *ao* value gives a lot higher production plateau than the new *aw* value for this time interval. They also give a slower, but sharper production curve where the production rate is slower in the beginning, but faster towards the end.

Based on the observations it was concluded (as expected) the the crossing point on the capillary pressure curve determines the production plateau, and it should be kept at around water saturations 0.68 to 0.69 as the residual oil saturation is $S_{or} = 0.311$.

By looking at figure 22b it can be seen that increasing *Aw* gives a faster production in the beginning than increasing *cw*, but the increasing *cw* gives a higher production plateau for the same time period, and this is due to it having a higher crossing point, on the water saturation axis, on the capillary pressure curve.

From both figure 22a and 22b it can be seen that the increase and decrease of *co* gives a relatively small change in production curve, but it gives a noticable change in production curve shape with slower production in beginning and faster in the end when doubled.

4.3 Simulations for match of 6 cm core

In order to see how the diffusion coefficient might affect the recovery of the experiments performed by Standnes one has to have a valid simulation model. In order to create a model which can be used to make an evaluation of the diffusion coefficient it is necessary to create a model that gives results that corresponds to the results that was observed in the experiments.

There were four experiments with four cores of different sizes to compare the simulation with. It was decided to first see if a match could be made with the core of 6cm diameter. This decision was made due to the fact that the smallest cores had such a rapid oil recovery due to their size that they might not have had time balance out any human errors during the start of the test. It is believed that a bigger core with more oil (and therefore more time to recover the oil) would have longer time to balance out any errors in the initial oil recovery.

After some modifications to the capillary pressure input variables the match between the simulation and the experimental test for the 6cm core was relatively close as can be seen in figure 23

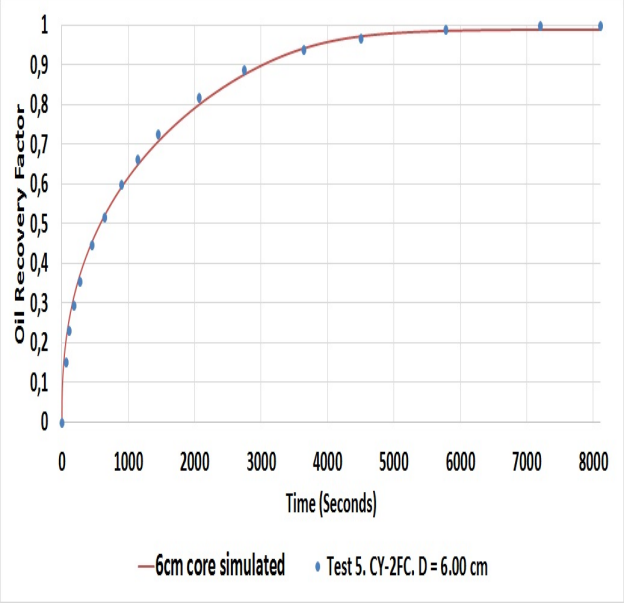

Figure 23: *A figure showing the recovery factor for the experimental test (the blue dots) and the simulated recovery factor from Eclipse (the red line).*

The relative permeability and capillary table used to get this match is displayed in table 3.

Table 3: *Relative permeability curves used throughout this thesis and the corresponding starting capillary pressure.*

Sw	krw	kro	Pc
0	0	1	12
0.02	4.87E-06	0.965553	8.290927
0.04	3.89E-05	0.931302	7.227273
0.06	0.000131	0.89725	6.643271
0.08	0.000312	0.863403	6.242495
0.1	0.000608	0.829767	5.937493
0.12	0.001051	0.796348	5.690806
0.14	0.001669	0.763151	5.483019
0.16	0.002492	0.730182	5.302795
0.18	0.003548	0.69745	5.142938
0.2	0.004867	0.664962	4.998591
0.22	0.006478	0.632725	4.86631
0.24	0.008411	0.600748	4.743549
0.26	0.010693	0.569041	4.628359
0.28	0.013356	0.537613	4.519194
0.3	0.016427	0.506476	4.414793
0.32	0.019936	0.475642	4.314088
0.34	0.023913	0.445124	4.216144
0.36	0.028386	0.414937	4.120114
0.38	0.033385	0.385097	4.025196
0.4	0.038938	0.355621	3.930599
0.42	0.045076	0.326531	3.835504
0.44	0.051827	0.297849	3.73903
0.46	0.05922	0.269602	3.640176
0.48	0.067285	0.241821	3.537759
0.5	0.076051	0.21454	3.430311
0.52	0.085547	0.187804	3.315931
0.54	0.095802	0.161663	3.192035
0.56	0.106846	0.136182	3.054922
0.58	0.118708	0.111444	2.898963
0.6	0.131416	0.087557	2.714904
0.62	0.145001	0.064677	2.485875
0.64	0.159491	0.043038	2.175949
0.66	0.174915	0.023055	1.684872
0.68	0.191303	0.005729	0.461248
0.688	0.198135	0.000419	-2.57547
0.689	0.199	0	-2.95506

It is not a 100% perfect match, but this can be due to uncertainties in the experiment and also the fact that it is believed that a match such as this can be created with alternative input values for No, Nw, Krw^*, Kro^*, Co, Cw, Aw and Ao.

The constants that are used for table 3 are displayed in table 4

nw	**no**	**krw***	**kro***	**cw**	**aw**	**co**	**ao**
3	1.19	0.199	1	6.55	0.14	-3.02	0.175

Table 4: *Values for the different parameters used to create table 3*

Now that the history match for the case of a $6cm$ core has been performed it would be of interest to use the same input parameters, for the relative permeabilities and capillary pressures, on the other cores in order to see if the simulation will match with the experimental data from the other three cores as well.

When testing the other cores table 4 was used, while the residual oil saturation was changed for each core with values given in table 1. This resulted in a slightly different relative permeability and capillary pressure table than the case in table 3 for each core. Other parameters that were changed between each core simulation were the porosity and grid of the core, although these had no effect on the relative permeabilities or the capillary pressure. The resulting simulations in comparison to the experimental observation for each core can be seen in figure 24.

As can be seen in figure 24 the input values that gave a decent match in the 6cm core gave a good match in the 1.99cm core (figure 24a), while on the other two cores of 3.49cm and 10cm cores the simulation produced a little bit too fast compared to the experimental data. This could possibly be explained by the fact that the cores are not 100% equal in terms of for example absolute permeability or the difference in experimental error between the different cores.

Due to the good match with the 6cm core and the fact that the 1.99cm core has such a short production time period it was decided to use the simulation for the 6cm core for the future work.

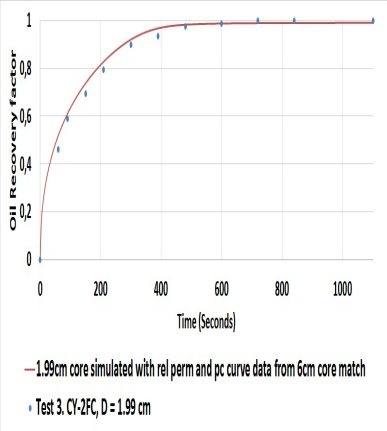

(a) *Figure showing the simulated recovery factor for oil (red line) along with the observed recovery factor from the experimental test versus time in seconds, for the 1.99cm diameter core.*

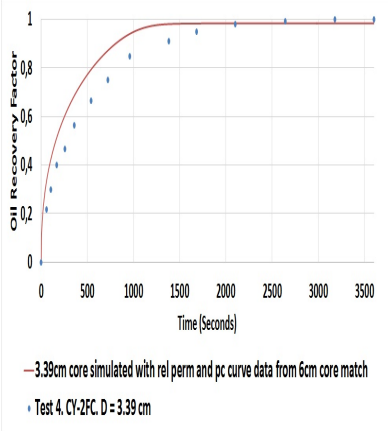

(b) *Figure showing the simulated recovery factor for oil (red line) along with the observed recovery factor from the experimental test versus time in seconds, for the 3.49cm diameter core.*

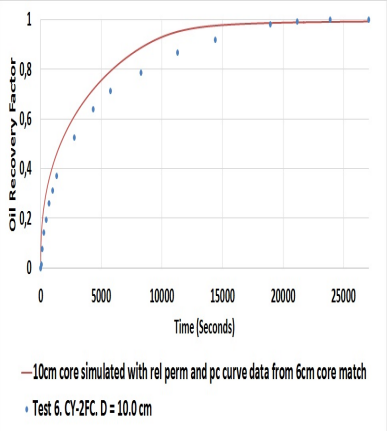

(c) *Figure showing the simulated recovery factor for oil (red line) along with the observed recovery factor from the experimental test versus time in seconds, for the 10cm diameter core.*

Figure 24

4.4 Tests for different values of D

In order to see if and how changes in the diffusion coefficient affects the simulated oil recovery rate, the coefficient has to be calculated first. The diffusion coefficient is calculated by the use of equation 2

$$D(S_w) = -\frac{Kk_{ro}}{\mu_o} \cdot \frac{1}{1 + \frac{k_{ro}}{k_{rw}} \cdot \frac{\mu_w}{\mu_o}} \frac{dP_c}{dS_w}$$

This equation gives a table of diffusion coefficient values at different saturations. The relative permeability and capillary pressures used to create this table are given previously in table 3. The approximated definition of a derivative from equation 32 is used which gives the following equation for the different derivatives of the capillary pressure:

$$\frac{\partial P}{\partial S_w} \approx \frac{P(S_{w2}) - P(S_{w1})}{S_{w2} - S_{w1}} \tag{36}$$

Sw	D(Sw)
0	DIV0
0.02	4.24E-18
0.04	4.55E-16
0.06	6.83E-15
0.08	4.64E-14
0.1	2.05E-13
0.12	6.92E-13
0.14	1.94E-12
0.16	4.75E-12
0.18	1.05E-11
0.2	2.15E-11
0.22	4.12E-11
0.24	7.5E-11
0.26	1.31E-10
0.28	2.2E-10
0.3	3.58E-10
0.32	5.69E-10
0.34	8.84E-10
0.36	1.35E-09
0.38	2.02E-09
0.4	3E-09
0.42	4.39E-09
0.44	6.37E-09
0.46	9.18E-09
0.48	1.31E-08
0.5	1.87E-08
0.52	2.66E-08
0.54	3.76E-08
0.56	5.3E-08
0.58	7.47E-08
0.6	1.05E-07
0.62	1.5E-07
0.64	2.22E-07
0.66	4.14E-07
0.68	9.7E-07
0.688	1.15E-07
0.689	0

Table 5: *A table that displays the calculated values of the diffusion equation.*

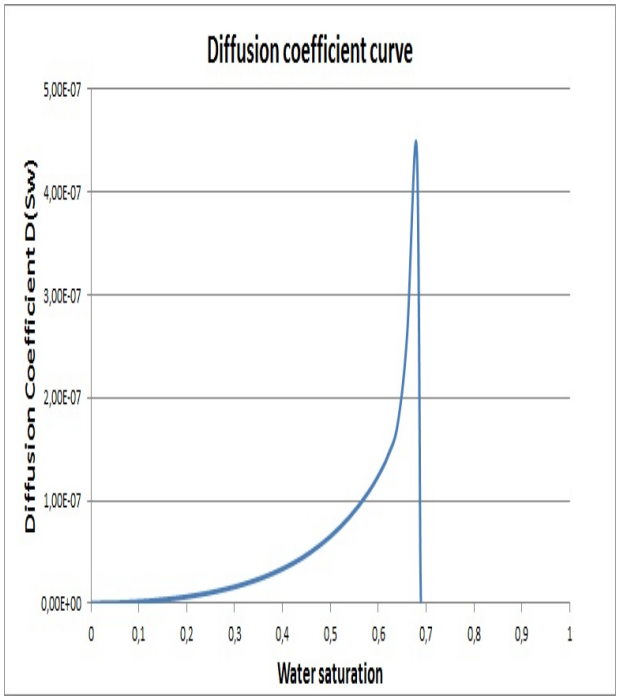

Figure 25: *Figure of the diffusion coefficient curve for the different water saturations in the core. For the 6cm core history match.*

The calculated values of the diffusion coefficient for the simulated match with the 6cm core is given in table 5.

The values in table 5 gives the graph given in figure 25 where it can be seen that the matched case is skewed quite far to the right on the water saturations. The water saturations end at around 0.689 due to the residual oil being 0.311.

The goal of the simulations is to see if the recovery of oil is dependant on the diffusion coefficient in some way and see how changes in the diffusion coefficient will affect the recovery factor. It was therefore decided to see what would happen with the recovery curve if the area under the diffusion coefficient graph from figure 25 was held constant while changing some of the input parameters that changes the shape of the diffusion coefficient curve.

The method used to estimate the area under the diffusion coefficient curve was the

trapezoid rule as discussed in section 2.7.1. This gave a relatively good estimation of the area as can be seen in figure 26

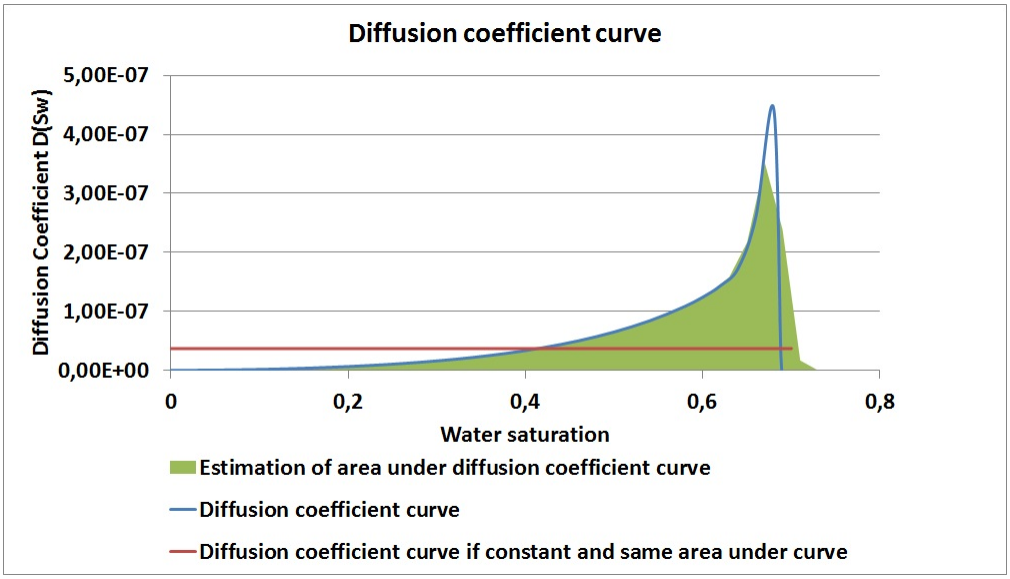

Figure 26: *The blue line represents the diffusion coefficient curve that gave the history match in the 6cm core. The green area is the estimated area under the diffusion coefficient curve with the use of the trapezoid rule. The red line represents the total area under the graph and is how the diffusion coefficient curve would look like if it was at a constant value throughout the whole water saturation interval.*

This method gave a value of $3.70E-8$ for the area under the diffusion curve.

4.4.1 Constant area under Diffusion curve

In this section it was decided to see if there would be any change in production profile if the area under the diffusion coefficient was held constant while changing the shape of the curve. It is observed that only the changes to the relative permeabilities and capillary pressure can change the shape of the diffusion curve, while input parameters such as absolute permeability can only affect the height of each point in the diffusion curve. Due to the capillary pressure curve being dependant on four different parameters it was decided to change the shape of the coefficient curve by changing the relative permeabilities. This was due to them being dependant on No and Nw and it would be easier to change one of these parameters and keep the area constant by changing the other one as well, as opposed to try to keep constant

area by changing four different parameters in the capillary pressure curve.

4.4.1.1 Changing No and Nw while holding Diffusion coefficient area constant

The initial value of the area under the curve was $3.70E-8$. When changing the values of No and Nw this area changes and getting a 100% match with the initial case would require going far into the decimal points in the No and Nw values. Due to this and the fact that the trapezoid rule is an estimation of the area it was decided to accept a difference of less than $1.0E-11$.

In order to get a decent amount of values it was decided to use values for No ranging from 1 to 6 while at the same time changing the Nw in order to hold the area under the graph constant for each given No value. It was observed that as soon as the value of No got to 3 and above the shape of the diffusion curve would become skewed to the left. When trying to see if there is a relationship between the shape of the diffusion curve and the production it is necessary to test out many different shapes of the curve and not only the left and right skewed cases, and so it was decided to increase the No value with 0.5 in the interval $1-3$ and then increase it with 1. This resulted in nine curves of the diffusion coefficient as can be seen in figure 27.

As can be seen in figure 27 the shape of the diffusion curve varies a lot for the different Nw and No values. The curve goes from a right skewed case to a more symmetrical case when the values are $No = 2$ and $Nw = 1.076$ and then moves over to a left skewed curve. This resulted in a few different relative permeability tables that was tested in the simulator. The simulated results for these different No and Nw values are given in figure 28

As can be seen in figure 28 the production varies a lot based on the different diffusion coefficient curves. This can be interpreted as the shape of the diffusion coefficient does have some impact on the production. It can also be seen that the initial match case is the only one with a decent match while every curve that is less skewed to the right gives a lower production at every point on the same timeline.

The only case that gives a comparable result with the initial match is the case where the diffusion curve is even more skewed to the right with $No = 1$ and $Nw = 7.61$. This last case gives a production that is less than the initial match up until about 4750 seconds in

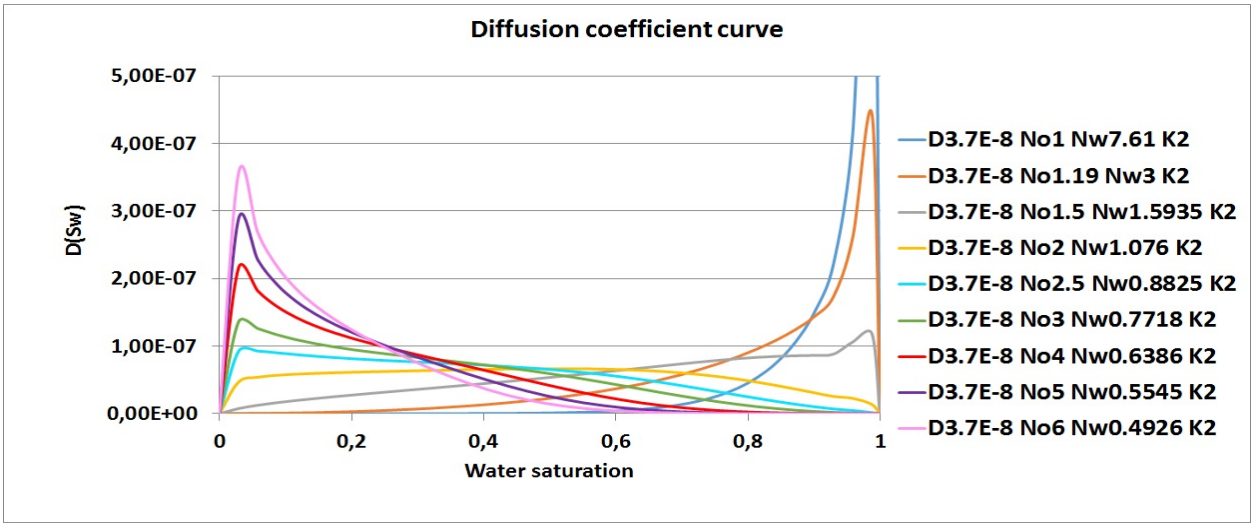

Figure 27: *The diffusion coefficient curves for different values of No (ranging from 1-6) and Nw (ranging from 0.4926-7.61), with a permeability (K) of 2 milli Darcy and a constant area under the graph of about 3.7 E-8.*

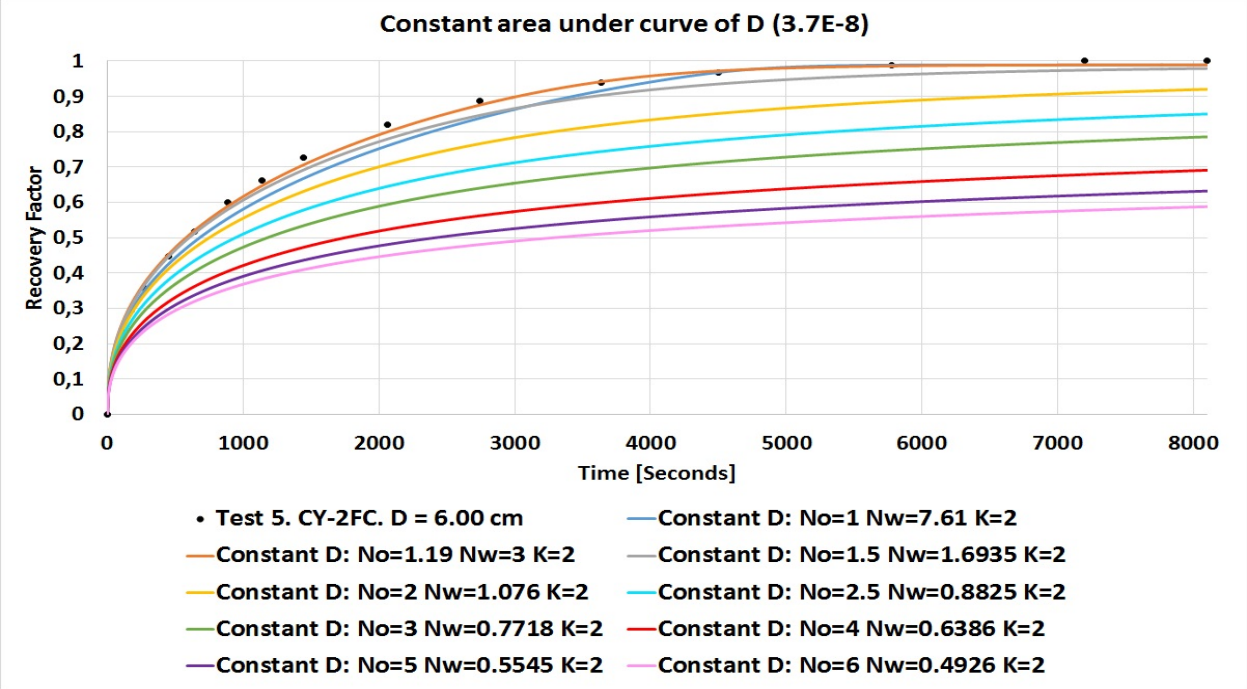

Figure 28: *The oil recovery factor versus time for the different diffusion coefficient curves given in figure 27. The curves in this production gives a representation of the simulation with the same colored curves in figure 27.*

the timeline, after which this new diffusion curve gives a faster production than the matched case.

The production curve for $No = 1$ and $Nw = 7.61$ is the only curve that has a different shape and crosses the other production curves. This could possibly be explained by the fact that the No and Nw values are supposed to stay within the range of 1-6. This curve also has a even more right skewed diffusion coefficient curve than the initial match.

4.4.1.2 Doubled area under the Diffusion coefficient curve

As it was seen in section 4.4.1.1 there was a change in the production rate when the shape of the diffusion curve changed. This happened regardless of the fact that the area under the cure was kept as a constant. Due to this it is now of interest to see if there is a relationship between the total area under the curve and the production rate or if it is only the shape of the curve that affects the production.

The same procedure was done in this section as in section 4.4.1.1, only this time the area under the curve that was used was doubled. The No and Nw values used were the same as in section 4.4.1.1, while the absolute permeability was doubled from 2mD to 4mD in order to get the doubled area under the diffusion coefficient curve. The results for the simulated production curves and the diffusion coefficient curves can be seen in figure 29.

As it can be observed in figure 29a the production profiles gives a faster production rate than the production profiles in figure 28. This can indicate that there is a relationship between the total area under the diffusion coefficient term and the production rate.

From this observation one can see that even though the production rate is increased for the doubled diffusion coefficient area, the shape of the production curve is different. This could imply that the shape of the diffusion coefficient has a bigger impact on how the production curve looks.

What can also be observed based on figure 29a is that if one look at for example the production curve for $No = 2$ and $Nw = 1.076$ the production at the beginning is faster than the experimental test while at a later time it is slower. This curve also ends up at a lower production than the experimental test for the same time interval. From this it seems like even though an increase in the diffusion coefficient gives an increase in production rate, it

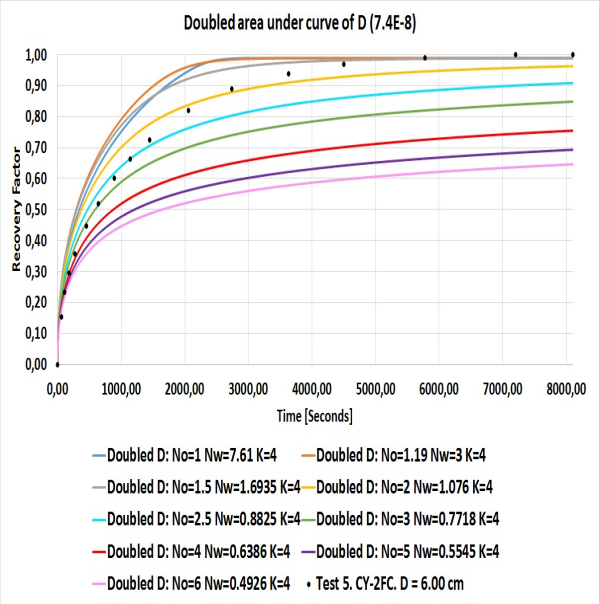

(a) *The production profiles for the different diffusion coefficient terms in 29b. The color of the production profile is the same as the color of the diffusion coefficient curve used to create it.*

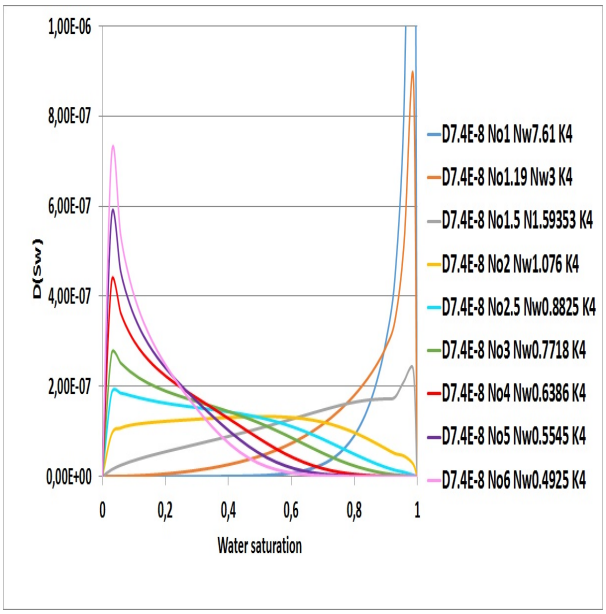

(b) *The diffusion coefficient curves where the total area under the curves is doubled from the area under the curve in section 4.4.1.1. Permeability is 4, No = 1 - 6, Nw = 0.4925 - 7.61.*

Figure 29: *The production curves that are obtained from the corresponding diffusion coefficient curves. The area under the coefficient curves are doubled (7.4E-8) from the area under the curve in section 4.4.1.1.*

does not look like an increase in total coefficient area is enough to replicate the initial match given by the right skewed coefficient curve. In other words it seems like the shape of the diffusion coefficient curve is the deciding factor when it comes to the shape of the production curve while the total area can change how fast each given case will reach its plateau.

4.4.1.3 Halved area under the Diffusion coefficient curve

As there was seen that the production rate was increased when the total area under the diffusion coefficient curve was increased it would be of interest to see if the opposite is true when the total area is decreased. This was done by keeping the same No and Nw values as in section 4.4.1.1 while cutting the absolute permeability in half (K=1mD). As the diffusion coefficient is linearly dependant on the absolute permeability this cuts the total area under

the curve in half. The simulated results for the halved diffusion coefficient curve is displayed in figure 30.

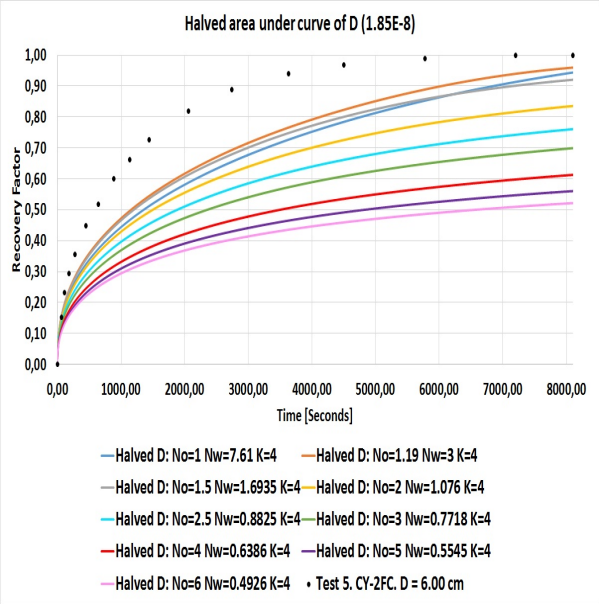

(a) *The production profiles for the different diffusion coefficient terms in 30b. The color of the production profile is the same as the color of the diffusion coefficient curve used to create it.*

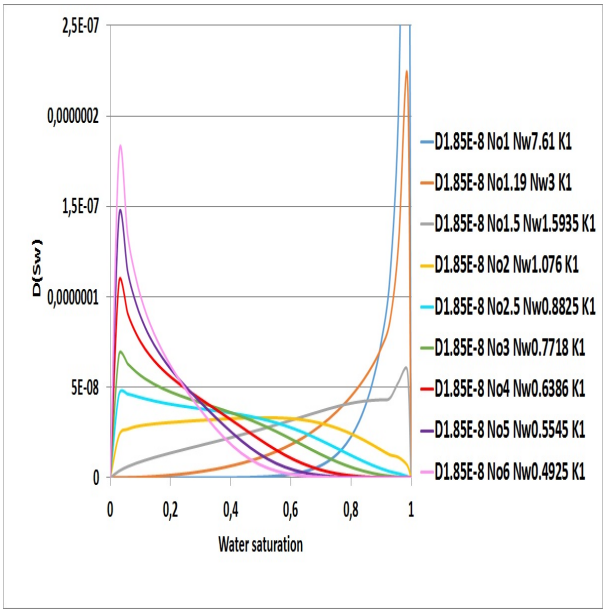

(b) *The diffusion coefficient curves where the total area under the curves is halved from the area under the curve in section 4.4.1.1. Permeability is 1, No = 1 - 6, Nw = 0.4925 - 7.61.*

Figure 30: *The production curves that are obtained from the corresponding diffusion coefficient curves. The area under the coefficient curves is halved (1.85E-8) from the area under the curve in section 4.4.1.1.*

The results from figure 30a shows that as suspected the production rate is decreased as there is a decreased total area under the diffusion coefficient curve. This further indicates that the total diffusion coefficient area has an impact on the production rate.

4.4.1.4 Comparing the different production profiles

As it was discovered that the production profiles varied depending on both the shape of the diffusion coefficient curve and on the total area underneath the curve it would be of interest to see how different the rates was. It was therefore decided to read of the time when each curve was at RF=0.5 and RF=0.8. These numbers were decided as all the curves are

Table 6: *A table illustrating the time it takes for each simulated case to reach RF=0.5 and how they compare to each other.*

NO	NW	Time [S] until RF=0.5 for total diffusion coefficient = 3.7E-8	Total diffusion coefficient area	% difference between time for No=1.19. Nw=3and new No and Nw values for D=3.7E-8	Time [S] until RF=0.5 for total diffusion coefficient = 7.4E-8	Total diffusion coefficient area	% difference between time for No=1.19. Nw=3 and new No and Nw values for D=7.4E-8	Time [S] until RF=0.5 for total diffusion coefficient =1.85E-8	Total diffusion coefficient area	% difference between time for No=1.19. Nw=3 and new No and Nw values for D=1.85E-8	Ratio time (D=7.4E-8)/(D=3.7E-8)	Ratio time (D=1.85E-8)/(D=3.7E-8)
1	7.61	666.00	3.69592573E-08	17.83	334.80	7.39185146E-08	17.72	1321.20	1.84796286E-08	17.25	0.50270271	1.983784
1.19	3	565.20	3.69613912E-08		284.40	7.39227823E-08		1126.80	1.84806956E-08		0.503184713	1.993631
1.5	1.5935	586.80	3.69611394E-08	3.82	295.20	7.39222788E-08	3.80	1173.60	1.84805697E-08	4.15	0.503067493	2.000000
2	1.076	730.80	3.69619071E-08	29.30	367.20	7.39238141E-08	29.11	1461.60	1.84809535E-08	29.71	0.502463054	2.000000
2.5	0.8825	918.00	3.69599754E-08	62.42	460.80	7.39199508E-08	62.03	1836.00	1.84799877E-08	62.94	0.501960817	2.000000
3	0.7718	1144.80	3.69607742E-08	102.55	576.00	7.39215483E-08	102.53	2289.60	1.84803871E-08	103.19	0.503144645	2.000000
4	0.6386	1692.00	3.69631803E-08	199.36	849.60	7.39263605E-08	198.73	3376.80	1.84815901E-08	199.68	0.502127665	1.995745
5	0.5545	2318.40	3.69571058E-08	310.19	1162.80	7.39142116E-08	308.86	4636.80	1.84785529E-08	311.50	0.501552795	2.000000
6	0.4925	3139.20	3.69629E-08	455.41	1569.60	7.39257E-08	451.90	6264.00	1.84845E-08	455.91	0.500000016	1.995413

relatively close to eachother in the beginning and spread out more and more as time moves. Also every production curve was able to get to RF=0.8 while not all of them managed to get to for example RF=0.9 for the length of these simulations. Two points where decided in order to see if any relationship between the curves would change as the curves got more spread out. The table 6 was produced and it can be seen that there is a relationship between the total area under the diffusion curve and the production curves. When the shape of the coefficient curve is kept the same (by using the same No and Nw input values) and the area underneath the coefficient curve is doubled then the production time to reach RF=0.5 is about halved. In the other case for when the area under the diffusion curve is halved then the time to reach RF=0.5 is doubled.

The percentage difference between the production curves of different No and Nw values and the initial values ($No = 1.19$ and $Nw = 3$) also stays roughly the same for each of the three cases of total area under the diffusion curve.

As it can be seen the time used to produce RF=0.5 is not exactly doubled or halved for either case. This might be explained by the fact that the area underneath the diffusion curve is not exactly doubled or halved as can be seen in table 6. The small differences can also be explained by reading error as the time for exactly RF=0.5 is not given by the simulator.

In order to get a more accurate picture of these observations it was decided to also see if

Table 7: *A table illustrating the time it takes for each simulated case to reach RF=0.5 and how they compare to each other.*

NO	NW	Time [S] until RF=0.8 for total diffusion coefficient = 3.7E-8	Total diffusion coefficient area	% difference between time for No=1.19. Nw=3and new No and Nw values for D=3.7E-8	Time [S] until RF=0.8 for total diffusion coefficient = 7.4E-8	Total diffusion coefficient area	% difference between time for No=1.19. Nw=3 and new No and Nw values for D=7.4E-8	Time [S] until RF=0.8 for total diffusion coefficient =1.85E-8	Total diffusion coefficient area	% difference between time for No=1.19. Nw=3 and new No and Nw values for D=1.85E-8	Ratio time (D=7.4E-8)/(D=3.7E-8)	Ratio time (D=1.85E-8)/(D=3.7E-8)
1	7.61	2347.20	3.69592573E-08	15.60	1177.20	7.39185146E-08	15.55	4687.20	1.84796286E-08	15.63	0.501533742	1.996933
1.19	3	2030.40	3.69613912E-08		1018.80	7.39227823E-08		4053.60	1.84806956E-08		0.50177305	1.996454
1.5	1.5935	2203.20	3.69611394E-08	8.51	1105.20	7.39222788E-08	8.48	4399.20	1.84805697E-08	8.53	0.501633987	1.996732
2	1.076	3196.80	3.69619071E-08	57.45	1602.00	7.39238141E-08	57.24	6386.40	1.84809535E-08	57.55	0.501126126	1.997748
2.5	0.8825	5148.00	3.69599754E-08	153.55	2577.60	7.39199508E-08	153.00	10281.60	1.84799877E-08	153.64	0.50069934	1.997203
3	0.7718	8877.60	3.69607742E-08	337.23	4442.40	7.39215483E-08	336.04	17784.00	1.84803871E-08	338.72	0.500405487	2.003244
4	0.6386	27792.00	3.69631803E-08	1268.79	13896.00	7.39263605E-08	1263.96	56160.00	1.84815901E-08	1285.44	0.500000018	2.020725
5	0.5545	71280.00	3.69571058E-08	3410.64	35280.00	7.39142116E-08	3362.90	141840.01	1.84785529E-08	3399.11	0.49494953	1.989899
6	0.4925	163440.01	3.69629E-08	7949.65	82080.00	7.39257398E-08	7956.54	326159.99	1.84845250E-08	7946.18	0.502202594	1.995595

the same oservations could be made for the case of production time at RF=0.8. As can be seen in table 7.

As can be seen in table 7 the same observations can be made in terms of time used to reach the same production for the initial case versus the double and halved coefficient area. The doubled area uses half the time and the halved area use twice as long.

4.4.2 Changing No and capillary pressure while holding diffusion coefficient area constant

Another study done to change the shape and peak location of the diffusion coefficient curve was to see if and how the relative oil permeability would change the production curve, while keeping the diffusion coefficient area constant. This was done by changing the input value No and then change the capillary pressure curve.

In order to make this comparison a bit easier than to change five different input variables (No, Cw, Aw, Co and Ao) it was decided to multiply the whole capillary pressure curve with a constant while changing the No value so that the diffusion coefficient curve area is kept constant. The capillary pressure curve was multiplied with values going from 0.5 to 4 while adjusting the No variable to keep the diffusion curve area constant. This would ensure that only the No variable would change the shape of the coefficient curve as the shape of

the capillary pressure was kept constant. Again the acceptable difference in total diffusion coefficient area was set to $1E-11$. Once these values was found and simulated it was of interest to see if there would be any change by increasing or decreasing the total diffusion coefficient area. This was again done by increasing and decreasing the absolute permeability to 4 and 1 respectively (where K=4 resulted in twice the area and K=1 in half the initial area).

As it can be seen in figure 31c and 31b the production curves where the PC is multiplied with 0.5 and 1 (where 1 gives the initial history match case) has roughly the same shape. The difference is that when the PC value is multiplied with 0.5 and $No = 0.834$ the production is slower until about 5700 seconds at which point the production is reaching its plateau for this time period. When the PC value is multiplied by numbers above 1 and the No value is adjusted accordingly above, 1.19, the production curves are all faster than the initial match case in the beginning. At the end however the initial case with $No = 1.19$ has the highest production end point for the given time interval. In other words, for the same time period, the higher the No value the lower the production plateau is. The change in production curve shape seems to be related to the change in coefficient curve shape. As when PC is multiplied by both 1 and 0.5 the corresponding No gives a very right skewed coefficient curve. For all other cases (when the production curves seems to change shape the most from the initial case) the coefficient curves goes more and more towards an even bell shaped curve.

As mentioned above the time to reach $RF = 0.5$ (as can be seen in table 8) is longest for the case of PC multiplied by 0.5 and second longest for the initial match case. The fastest production curve for $RF = 0.5$ seems to be when PC is multiplied by 2 and $No = 1.704$ and values above this starts to produce slower again. These observations are valid also for the case of a doubled and halved area under the diffusion curve, which also can be seen in table 8.

When it comes to the higher production numbers such as the $RF = 0.8$ the time to reach this production is still the longest for the case of PC multiplied by 0.5 and $No = 0.834$. Here again there are a few curves that are faster than the initial curve of $No = 1.19$, but the difference is less than in the case for $RF = 0.5$. As can be seen in table 8 the difference between the $No = 1.19$ and the fastest curve $No = 1.704$ for the $RF = 0.5$ case is 10.56%.

Table 8: *A table illustrating the time it takes for each simulated case to reach RF=0.5 and how they compare to each other.*

PC	NO	Time [S] until RF=0.5 for total diffusion coefficient = 3.7E-8	Total diffusion coefficient area	% difference between time for PC*1, No=1.19 and new PC and No values for D=3.7E-8	Time [S] until RF=0.5 for total diffusion coefficient = 7.4E-8	Total diffusion coefficient area	% difference between time for PC*1, No=1.19 and new PC and No values for D=7.4E-8	Time [S] until RF=0.5 for total diffusion coefficient =1.85E-8	Total diffusion coefficient area	% difference between time for PC*1, No=1.19 and new PC and No values for D=1.85E-8	Ratio time (D=3.7E-8)/(D=7.4E-8)	Ratio time (D=3.7E-8)/(D=1.85E-8)
0.5	0.834	738.00	3.69619E-08	27.33	370.80	7.39239E-08	27.16	1468.80	1.84810E-08	27.10	1.99	0.502
1	1.19	579.60	3.69614E-08		291.60	7.39228E-08		1155.60	1.84807E-08		1.99	0.502
1.5	1.461	529.20	3.69615E-08	8.70	266.40	7.39230E-08	8.64	1058.40	1.84808E-08	8.41	1.99	0.500
2	1.704	518.40	3.69599E-08	10.56	259.20	7.39197E-08	11.11	1029.60	1.84799E-08	10.90	2.00	0.503
2.5	1.933	522.00	3.69595E-08	9.94	262.80	7.39191E-08	9.88	1036.80	1.84798E-08	10.28	1.99	0.503
3	2.1524	529.20	3.69604E-08	8.70	266.40	7.39208E-08	8.64	1054.80	1.84802E-08	8.72	1.99	0.502
3.5	2.3637	540.00	3.69625E-08	6.83	273.60	7.39250E-08	6.17	1076.40	1.84813E-08	6.85	1.97	0.502
4	2.5678	558.00	3.69607E-08	3.73	280.80	7.39213E-08	3.70	1108.80	1.84803E-08	4.05	1.99	0.503

Table 9: *A table illustrating the time it takes for each simulated case to reach RF=0.5 and how they compare to each other.*

PC	NO	Time [S] until RF=0.8 for total diffusion coefficient = 3.7E-8	Total diffusion coefficient area	% difference between time for PC*1, No=1.19 and new PC and No values for D=3.7E-8	Time [S] until RF=0.8 for total diffusion coefficient = 7.4E-8	Total diffusion coefficient area	% difference between time for PC*1, No=1.19 and new PC and No values for D=7.4E-8	Time [S] until RF=0.8 for total diffusion coefficient =1.85E-8	Total diffusion coefficient area	% difference between time for PC*1, No=1.19 and new PC and No values for D=1.85E-8	Ratio time (D=3.7E-8)/(D=7.4E-8)	Ratio time (D=3.7E-8)/(D=1.85E-8)
0.5	0.834	2534.40	3.69619E-08	22.65	1267.20	7.39239E-08	22.65	5061.60	1.84810E-08	22.69	2.00	0.501
1	1.19	2066.40	3.69614E-08		1033.20	7.39228E-08		4125.60	1.84807E-08		2.00	0.501
1.5	1.461	1944.00	3.69615E-08	5.92	972.00	7.39230E-08	5.92	3873.60	1.84808E-08	6.11	2.00	0.502
2	1.704	1936.80	3.69599E-08	6.27	968.40	7.39197E-08	6.27	3859.20	1.84799E-08	6.46	2.00	0.502
2.5	1.933	1987.20	3.69595E-08	3.83	997.20	7.39191E-08	3.48	3974.40	1.84798E-08	3.66	1.99	0.500
3	2.1524	2066.40	3.69604E-08	0.00	1036.80	7.39208E-08	0.35	4125.60	1.84802E-08	0.00	1.99	0.501
3.5	2.3637	2188.80	3.69625E-08	5.92	1098.00	7.39250E-08	6.27	4370.40	1.84813E-08	5.93	1.99	0.501
4	2.5678	2347.20	3.69607E-08	13.59	1177.20	7.39213E-08	13.94	4687.20	1.84803E-08	13.61	1.99	0.501

While looking in table 9 the difference between the same curves for $RF = 0.8$ is reduced to 6.27%. It can also be seen from figure 31b that the $No = 1.19$ curve has the highest production and it is also the fastest to reach productions of $RF = 0.94$ and above.

These observations of which input values gives faster $RF = 0.5$ and $RF = 0.8$ productions are valid also for the doubled and halved diffusion curve area cases. The difference is that the initial area uses about twice as long for both $RF = 0.5$ and $RF = 0.8$ than the curves of the doubled diffusion curve area. The opposite is true when the diffusion curve area is halved. In this case the production curves from the initial diffusion area uses half the time for both $RF = 0.5$ and $RF = 0.8$ as opposed to the production curves achieved with halved diffusion curve area.

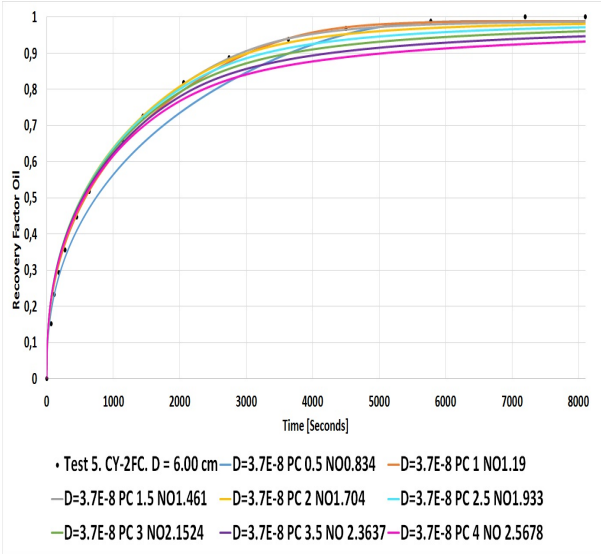

(a) *A figure showing the production curves of the different values for the changed No and PC values. Where the PC curve has been multiplied with a given value.*

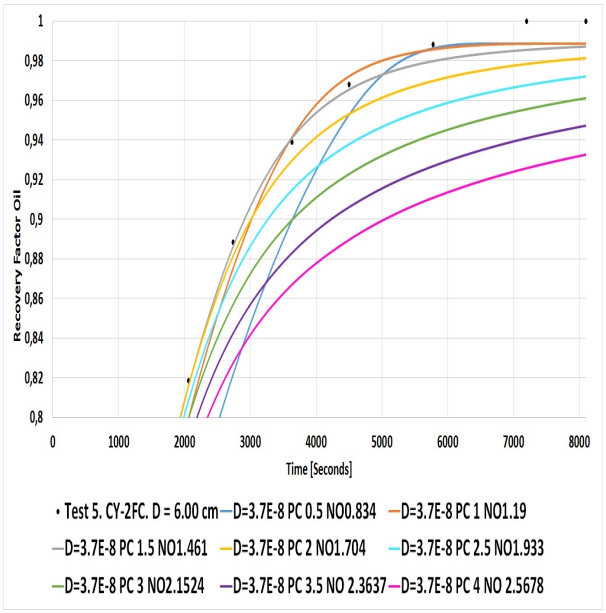

(b) *A zoomed in display of figure 31a that shows more detailed how the production curves varies towards the end.*

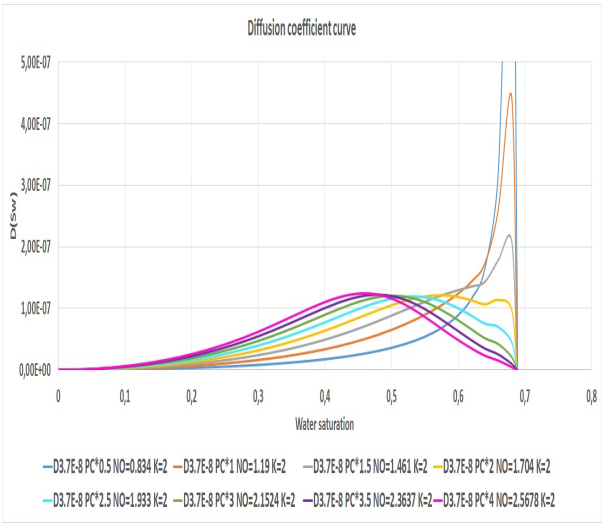

(c) *A figure showing the diffusion coefficient curve given by the different PC and No values. All of the curves have approximately the same area underneath them.*

Figure 31

4.4.3 Changing Nw and capillary pressure while holding Diffusion coefficient area constant

A study to see how the production curves would change if only the peak height of the diffusion curve changed was also conducted. In order to achieve such a study the No value was kept the same while multiplying the PC curve with a number and change the Nw input value in so that the area under the diffusion curve was kept constant. The PC curve was multiplied with values between 0.5 and 1.5. The reason for this was that in order to keep the diffusion curve area constant while multiplying the PC curve would require a Nw above 6 for PC multiplied with 1.5 and less than 1 for PC multiplied with 0.5. As mentioned in section 2.4 the corey exponents has a range from 1 to 6.

The diffusion coefficient curve is changed by multiplying the PC curve with a constant which will change the diffusion curve area. This change in curve area is counteracted by increasing the Nw value. When changing both the No and Nw values in section 4.4.1.1 it was discovered that changing the Nw values only affect the shape of the first part of the diffusion curve. As one can see from the diffusion curves in figure 32c the higher the Nw value the lower the diffusion curve values are for the lower water saturations. At the same time the higher the PC curve value the higher the diffusion curve peak becomes.

When looking at figure 32a and 32b it can be seen that the production curves created with $Nw = 0.861$, 1.1855, and 1.968 has a relatively slower production curve as opposed to the initial match with $Nw = 3$. The production curves created with PC multiplied with 1.1 to 1.4 and $Nw > 3$ seems to have a relatively similar production curve as the initial match of $Nw = 3$. They all seem to end up at the same production plateau which is not the case for the simulations done when changing the Nw and No or the PC and No values. This could indicate that the shape of the diffusion curve (and the peak location in terms of where it is placed on the water saturation axis) has more to say for the production plateau in the given time period, rather than the height of the diffusion curve peak.

It can be seen that all of the curves seems to have a relatively similar production rate at the beginning up to about $RF = 0.3$ before they spread out a bit more and then come together again at about $RF = 0.99$.

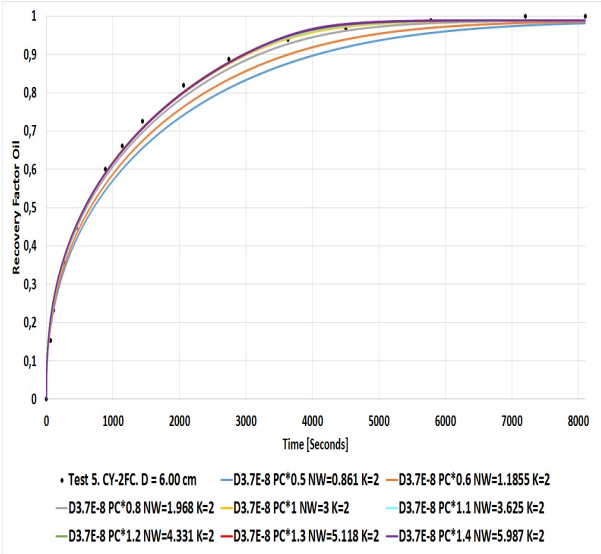

(a) *A figure showing the production curves of the different values for the changed Nw and PC values. Where the PC curve has been multiplied with a given value.*

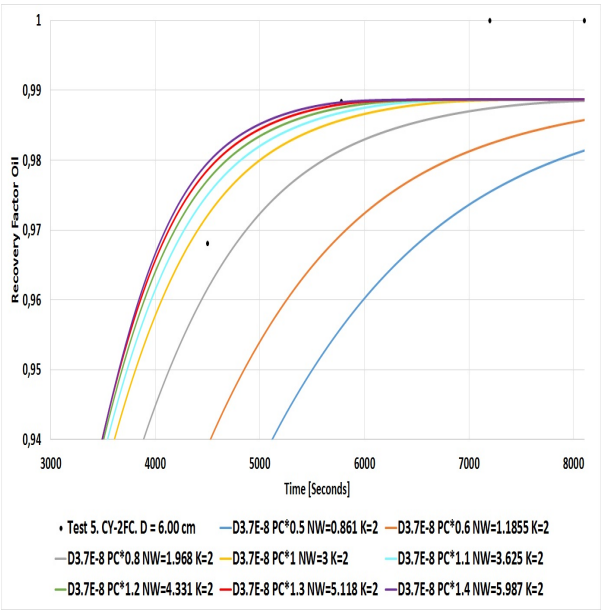

(b) *A zoomed in display of figure 32a that shows more detailed how the production curves varies towards the end.*

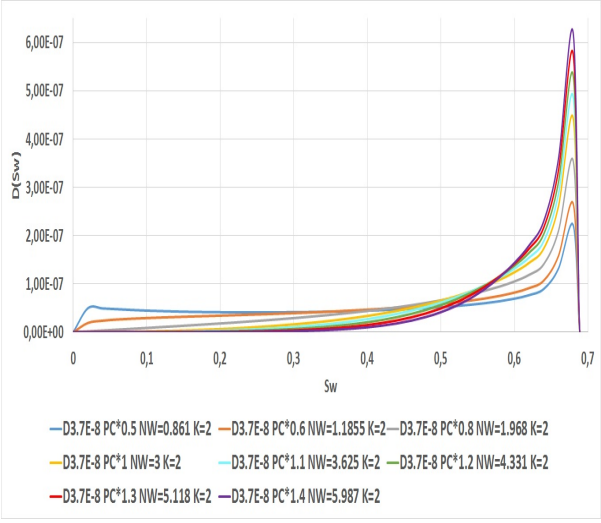

(c) *A figure showing the diffusion coefficient curve given by the different PC and Nw values. All of the curves have approximately the same area underneath them.*

Figure 32

It can be seen from table 10 that the time to reach $RF = 0.5$ is relatively longer for the cases where the PC is multiplied with a value less than 1 and the resulting NW is less than 3. The other curves however seem to have a relatively similar production time to reach $RF = 0.5$ where the biggest difference is only 7.2 seconds between the $Nw = 3$ and $Nw = 5.118$ curves. This seems to be true also for the curves created with a doubled and halved diffusion curve area. Again the production time to reach $RF = 0.5$ is about 2 times as long for the initial diffusion curve area as opposed to the doubled diffusion curve area. The opposite is true for the halved area where the initial diffusion curve area uses half the time to that the halved diffusion curve area use to reach $RF = 0.5$.

When looking at table 11 which shows times for reaching $RF = 0.8$ it can be seen that also here there is a relatively similar time to reach $RF = 0.8$ for the curves created with $Nw = 3$ and above. The time needed to reach $RF = 0.8$ is again relatively longer for the curves created with Nw values less than 3. Again the same trends are seen in the curves for the doubled and halved diffusion curve area. Again the initial area curves uses about twice as long as the doubled area curves to reach $RF = 0.8$, while the initial area curves uses half the time that the halved area curves uses to get to $RF = 0.8$.

Table 10: *A table illustrating the time it takes for each simulated case to reach RF=0.5 and how they compare to each other.*

PC	NW	Time [S] until RF=0.5 for total diffusion coefficient = 3.7E-8	Total diffusion coefficient area	% difference between time for PC*1, Nw=3 and new PC and Nw values for D=3.7E-8	Time [Seconds] until RF=0.5 for total diffusion coefficient = 7.4E-8	Total diffusion coefficient area	% difference between time for PC*1, Nw=3 and new PC and Nw values for D=7.4E-8	Time [S] until RF=0.5 for total diffusion coefficient =1.85E-8	Total diffusion coefficient area	% difference between time for PC*1, Nw=3 and new PC and Nw values for D=1.85E-8	Ratio time (D=3.7E-8)/(D=7.4E-8)	Ratio time (D=3.7E-8)/(D=1.85E-8)
0.5	0.861	709.20	3.696E-08	7.65	356.40	7.39256106E-08	7.61	1414.80	1.848140E-08	7.67	1.99	0.501272
0.6	1.1855	658.80	3.696E-08		331.20	7.39227823E-08		1314.00	1.848070E-08		1.99	0.501370
0.8	1.968	604.80	3.696E-08	8.20	302.40	7.39225854E-08	8.70	1202.40	1.848011E-08	8.49	2.00	0.502994
1	3	579.60	3.696E-08	12.02	291.60	7.39217088E-08	11.96	1155.60	1.848152E-08	12.05	1.99	0.501558
1.1	3.626	576.00	3.696E-08	12.57	288.00	7.39261213E-08	13.04	1144.80	1.847902E-08	12.88	2.00	0.503145
1.2	4.331	572.40	3.696E-08	13.11	288.00	7.39254082E-08	13.04	1141.20	1.848123E-08	13.15	1.99	0.501577
1.3	5.118	572.40	3.696E-08	13.11	288.00	7.39193980E-08	13.04	1141.20	1.848080E-08	13.15	1.99	0.501577
1.4	5.987	576.00	3.696E-08	12.57	291.60	7.39215653E-08	11.96	1148.40	1.848039E-08	12.60	1.98	0.501567

Table 11: *A table illustrating the time it takes for each simulated case to reach RF=0.8 and how they compare to each other.*

PC	NW	Time [S] until RF=0.8 for total diffusion coefficient = 3.7E-8	Total diffusion coefficient area	% difference between time for PC*1, Nw=3 and new PC and Nw values for D=3.7E-8	Time [S] until RF=0.8 for total diffusion coefficient = 7.4E-8	Total diffusion coefficient area	% difference between time for PC*1, Nw=3 and new PC and Nw values for D=7.4E-8	Time [S] until RF=0.8 for total diffusion coefficient =1.85E-8	Total diffusion coefficient area	% difference between time for PC*1, Nw=3 and new PC and Nw values for D=1.85E-8	Ratio time (D=3.7E-8)/(D=7.4E-8)	Ratio time (D=3.7E-8)/(D=1.85E-8)
0.5	0.861	2613.60	3.696E-08	9.67	1306.80	7.39256106E-08	9.67	5212.80	1.848140E-08	9.70	2.00	0.501381
0.6	1.1855	2383.20	3.696E-08		1191.60	7.39227823E-08		4752.00	1.848070E-08		2.00	0.501515
0.8	1.968	2152.80	3.696E-08	9.67	1076.40	7.39225854E-08	9.67	4298.40	1.848011E-08	9.55	2.00	0.500838
1	3	2066.40	3.696E-08	13.29	1033.20	7.39217088E-08	13.29	4125.60	1.848152E-08	13.18	2.00	0.500873
1.1	3.626	2052.00	3.696E-08	13.90	1026.00	7.39261213E-08	13.90	4096.80	1.847902E-08	13.79	2.00	0.500879
1.2	4.331	2044.80	3.696E-08	14.20	1022.40	7.39254082E-08	14.20	4082.40	1.848123E-08	14.09	2.00	0.500882
1.3	5.118	2052.00	3.696E-08	13.90	1026.00	7.39193980E-08	13.90	4089.60	1.848080E-08	13.94	2.00	0.501761
1.4	5.987	2059.20	3.696E-08	13.60	1029.60	7.39215653E-08	13.60	4111.20	1.848039E-08	13.48	2.00	0.500876

5 Conclusions

The questions in the beginning of this thesis was if there was a relationship between the diffusion coefficient in the imbibition equation and the production rate and how this relationship was. Could the diffusion coefficient be held constant and give the same production curve or did the change in diffusion coefficient due to different water saturations affect the production rate?

As discussed in section 4.4.1 it could be observed that both the total area under the diffusion coefficient curve and the shape of it had an effect on the production curve. In the simulations done for a 6 cm core and $S_{or} = 0.311$ it was observed that the change in production rate was relatively small when the diffusion curve peak was increased while keeping the shape the same.

When the No was changed and the shape changed more and more the simulated production curves started to give a more spread out plot indicating that the shape of the diffusion coefficient curve had a relatively big impact on the production.

When both the No and Nw values where changed while keeping the diffusion curve area constant the results showed that the production curves had a relatively high degree of difference as the shape of the diffusion curve changed.

When changing Nw and holding No constant the shape of the coefficient curve was kept relatively similar for all cases. The only difference was the height of the peak, and the resulting simulations gave relatively similar production curves.

It is then concluded that for the case discussed in this thesis that the shape of the diffusion curve has a big impact on how the production profile looks. A more right shifted diffusion coefficient curve gives the highest production while a more bell shaped and left shifted gives both a slower production rate and a lower total production for the same time period.

It could also be concluded that for the right shifted curve the only difference between a lower peak and the higher peak with the same total diffusion coefficient area was the rate of the production. As long as the shape stays the same the same production plateau will be reached, but a higher peak gives a higher production rate which reaches this plateau faster.

In the end it could also be observed that the total diffusion coefficient area had an affect

on the production curve as well. For all the simulated cases it could be seen that a doubling of the diffusion coefficient area gave a production rate that was twice as high as the initial diffusion curve area. The opposite is true when the diffusion curve area was divided by two. In this case it could be seen, for all simulations, that the production rate was cut in half and resulted in curves that used twice as long to reach the same recovery factor as the initial diffusion curve area.

6 Future work

It was concluded that both the shape and size of the diffusion coefficient term had an effect on the production curve. It would however be of interest to see how different parameters affects the shape and size of the coefficient term. In this thesis one capillary pressure curve was found and the shape of this was kept constant for all simulations. Is there a specific shape of the capillary pressure curve that is more beneficial than another and how would different end points for the relative permeabilities affect the diffusion coefficient curve and oil production?

It could also be of interest to see how a change in diffusion coefficient shape by changing the shape of capillary pressure curve would affect the production curve with constant water and oil relative permeabilities. Would this give similar results as when the coefficient shape was changed by keeping the capillary pressure curve constant and changing the relative permeabilities?

List of Abbreviations

μ Viscosity

μ_o Oil viscosity

μ_w Water viscosity

ϕ Porosity

ρ Fluid density

σ The interfacial tension between two immiscible fluids.

A Cross sectional area

A_c The cross sectional area of the capillary tube.

D Diffusion coefficient

I_o Ratio of spontaneous imbibition to total saturation change for oil

I_w Ratio of spontaneous imbibition to total saturation change for water

K Absolute permeability

$k_{rg,max}$ Maximum relative permeability of gas

k_{rg} Relative permeability of gas

$k_{ro,max}$ Maximum relative permeability of oil

k_{ro} Relative permeability of oil

$k_{rw,max}$ The maximum relative permeability of water

k_{rw} Relative permeability of water

L Distance

n_g Corey gas exponent

n_o Corey oil exponent

n_w Corey water exponent

P Pressure

Q Fluid flow rate

r_c The radius of the capillary tube.

S Normalized oil saturation

S_g Gas saturation

S_o Oil saturation

S_w Water saturation

S_{gc} Connate gas saturation

S_{or} Residual oil saturation

S_{wc} Connate water saturation

S_{wi} Initial water saturation

S_{wor} Water saturation after forced water flooding

S_{wos} Water saturation after uptake of oil

S_{wr} Water saturation forced oil flooding

S_{ws} Water saturation after SI

t Time

u Fluid velocity

u_o Oil velocity

u_w Water velocity

x Position in x coordinate

y Position in y coordinate

z Position in z coordinate

References

[1] Abdallah, W., Buckley, S. J., Carnegie, A., Herold, J., Edwards, J., Fordham, E., Graue, A., Habashy, T., Seleznev, N., Sidner, C., Hussain, H., Montaron, B., Ziauddin, M., 2007. Fundamentals of Wettability. Schlumberger, Oilfield Review.

[2] Anderson, W.G., 1986. Wettability Literature Survey - Part 2: Wettability Measurements. Journal of Petroleum Technology, pp. 1246-1262.

[3] Anderson, W.G., 1987. Wettability Literature Survey - Part 4: Effects of Wettability on Capillary Pressure. Journal of Petroleum Technology, pp. 1283-1300.

[4] Anderson, W.G., 1987. Wettability Literature Survey - Part 5: The Effects of Wettability on Relative Permeability. Journal of Petroleum Technology, pp. 1453-1468.

[5] Chen, Q., Butler, K.E., Gingras, M.K., Balcom, B.J., 2005. A mechanism study of co-current and counter-current imbibition using new magnetic resonance techniques. This paper was prepared for presentation at the International Symposium of the Society of Core Analysts held in Toronto, Canada, 21-25 August 2005.

[6] Green, D.W., Willhite, G.P., 1998. Enhanced oil recovery. SPE textbook series vol 6.

[7] Gupta, A., 2015. Numerical Methods using Matlab. Springer

[8] Kantzas, A., Pow, M., Allsopp, K., Marentette, D., 1997. Co-current and counter-current imbibition analysis for tight fractured carbonate gas reservoirs. PETROLEUM SOCIETY OF CIM, PAPER NO. 97-181.

[9] Kashciev, D., Firoozabadi, A., 2003. Analytical Solutions for 1D Countercurrent Imbibition in Water-Wet Media. SPE Journal pp. 401-408.

[10] Moe, M., 2016. Bachelor Thesis University of Stavanger Norway: Numerical investigation of the effect of sample shape and no-flow boundary conditions on the rate of spontaneous imbibition into short core samples.

[11] Morrow, N.R., 1990. Wettability and its effect on oil recovery. Journal of Petroleum Technology pp. 1476-1484.

[12] Morrow, N.R., Mason, G., 2001. Recovery of oil by spontaneous imbibition. Current Opinion in Colloid and Interface Science, 6, 321-337

[13] Qasem, F.H., Nashawi, I.S., Gharbi, R., Mir, M.I., 2008. Recovery performance of partially fractured reservoirs by capillary imbibition. Journal of Petroleum Science and Engineering, 60, 39-50.

[14] Skjaeveland, S.M., Siqveland, L.M., Kjosavik, A., Hammervold, T.W.L., Virnovsky, G.A., 2000. Capillary Pressure Correlation for Mixed-Wet Reservoirs. SPE Reservoir Eval. and Eng., 3 (1) pp. 60-67

[15] Standnes, D.C, 2006. Spontaneous imbibition of water into cylindrical cores with high aspect ratio: Numerical and experimental results. Journal of Petroleum Science and Engineering, 50, pp. 151–160.

[16] Tveito, A., Winther, R., 2008. Introduction to Partial Differential Equations. A Computational Approach. Springer-Verlag Berlin Heidelberg.

[17] Unsal, E., Mason, G., Morrow, N.R., Ruth, D. W., 2007. Co-current and counter-current imbibition in independent tubes of non-axisymmetric geometry. Journal of Colloid and Interface Science, 306, 105–117.

[18] Weber, K.J., 1982. Influence of common sedimentary structures on fluid flow in reservoir models. Journal of Petroleum Technology, 34 (03), pp. 665-672

[19] Zhang, D.L, Liu S., Puerto, M., Miller, C.A., Hirasaki, G.J., 2006. Wettability alteration and spontaneous imbibition in oil-wet carbonate formations. Journal of Petroleum Science and Engineering 52, 213–226.

[20] Zhou, D., Jia, L., Kamath, J., Kovscek, A.R., 2001. An Investigation of Counter-Current Imbibition Processes in Diatomite. SPE 68837.

[21] Zolotukhin, A.B., Ursin, JR., 2000. Introduction to petroleum reservoir engineering. Høyskoleforlaget.

[22] [cited 12.01.2017] http://www.glossary.oilfield.slb.com/Terms/w/wettability.aspx

[23] [cited 25.01.2017] http://www.vinci-technologies.com/products-explo.aspx?IDM=753995&IDR=82290&IDR2=113133

[24] [cited 02.02.2017] http://tutorial.math.lamar.edu/Classes/CalcII/ApproximatingDefIntegrals.aspx

[25] [cited 04.02.2017] http://www.glossary.oilfield.slb.com/en/Terms/p/permeability.aspx

[26] [cited 04.02.2017] http://www.fekete.com/SAN/WebHelp/FeketeHarmony/Harmony_WebHelp/Content/HTML_Files/Reference_Material/General_Concepts/Relative_Permeability.htm

[27] [cited 05.02.2017] http://petrowiki.org/Relative_permeability_models

[28] [cited 06.03.2017] http://tutorial.math.lamar.edu/Classes/CalcI/DefnOfDerivative.aspx

[29] [cited 28.03.2017] http://www.epgeology.com/reservoir-engineering-f10/wettability-oil-and-gas-reservoirs-t5978.html

[30] [cited 04.05.2017] http://www.fekete.com/SAN/WebHelp/FeketeHarmony/Harmony_WebHelp/Content/HTML_Files/Reference_Material/General_Concepts/Capillary_Pressure.htm

[31] [cited 20.05.2017] http://petrowiki.org/Recognizing_naturally_fractured_reservoirs

[32] [cited 27.05.2017] https://www.slb.com/resources/oilfield_review/~/media/Files/resources/oilfield_review/ors14/aut14/define_perm.ashx

7 Appendix

A TABLES

Table 12: *A table illustrating the difference between the achieved relative permeabilitiy and capillary table by attempting to match them to Moes table.*

Curves from own input data				Data from Moes paper				Difference between Moe data and own curves		
Sw	Match krw	Match kro	Pc	Sw	krw	kro	Pc	Krw Difference	Kro Difference	Pc Difference
0	0	1	12	0	0	1	12	0	0	0
0,02	4,86727E-06	0,965553197	8,838996	0,02	9,87E-06	0,963674	8,689549	5E-06	0,00188	0,149447
0,04	3,89382E-05	0,931301527	5,6086	0,04	9,9E-05	0,927626	7,489063	6E-05	0,003676	1,880463
0,06	0,000131416	0,897249849	4,292402	0,06	0,000432	0,899863	5,321871	0,0003	0,002613	1,029469
0,08	0,000311505	0,8634033	3,546962	0,08	0,000712	0,866392	3,879696	0,0004	0,002989	0,332734
0,1	0,000608409	0,829767321	3,056598	0,1	0,000909	0,83022	3,073528	0,0003	0,000453	0,016929
0,12	0,00105133	0,796347687	2,704694	0,12	0,001252	0,796355	2,953348	0,000201	6,88E-06	0,248654
0,14	0,001669473	0,76315054	2,43725	0,14	0,001971	0,761803	2,528805	0,000301	0,001347	0,091555
0,16	0,002492042	0,730182425	2,225521	0,16	0,002494	0,720574	2,335145	1,65E-06	0,009608	0,109624
0,18	0,003548239	0,697450335	2,052666	0,18	0,003551	0,683677	2,028708	2,35E-06	0,013773	0,023959
0,2	0,00486727	0,664961756	1,908099	0,2	0,00487	0,650121	1,832899	3,22E-06	0,01484	0,0752
0,22	0,006478336	0,632724729	1,784793	0,22	0,006483	0,616917	1,74212	4,29E-06	0,015807	0,042672
0,24	0,008410642	0,600747914	1,677878	0,24	0,008416	0,584076	1,714346	5,57E-06	0,016672	0,036469
0,26	0,010693391	0,569040666	1,583853	0,26	0,0107	0,551609	1,619808	7,08E-06	0,017432	0,035955
0,28	0,013355788	0,537613125	1,500123	0,28	0,013365	0,519529	1,495964	8,84E-06	0,018084	0,00416
0,3	0,016427035	0,506476328	1,424706	0,3	0,016438	0,487851	1,403134	1,09E-05	0,018625	0,021573
0,32	0,019936336	0,475642334	1,35605	0,32	0,01995	0,466589	1,349533	1,32E-05	0,009053	0,006517
0,34	0,023912895	0,445124382	1,292904	0,34	0,023929	0,445761	1,266437	1,58E-05	0,000636	0,026467
0,36	0,028385916	0,414937078	1,234229	0,36	0,028405	0,425383	1,191988	1,88E-05	0,010446	0,042241
0,38	0,033384602	0,385096629	1,179135	0,38	0,033407	0,385478	1,124688	2,21E-05	0,000381	0,054447
0,4	0,038938156	0,355621131	1,126824	0,4	0,038964	0,366066	1,063299	2,58E-05	0,010445	0,063525
0,42	0,045075783	0,32653094	1,076549	0,42	0,045106	0,337173	1,006766	2,98E-05	0,010642	0,069783
0,44	0,051826686	0,297849139	1,027562	0,44	0,051861	0,318828	0,954147	3,43E-05	0,020979	0,073415
0,46	0,059220069	0,269602149	0,979069	0,46	0,059259	0,281062	0,90456	3,92E-05	0,01146	0,074508
0,48	0,067285134	0,241820551	0,930155	0,48	0,06733	0,253913	0,857108	4,45E-05	0,012093	0,073047
0,5	0,076051087	0,214540196	0,879688	0,5	0,076101	0,228424	0,810794	5,03E-05	0,013884	0,068893
0,52	0,08554713	0,187803769	0,826154	0,52	0,085604	0,197456	0,764383	5,66E-05	0,009652	0,061771
0,54	0,095802466	0,161663056	0,767372	0,54	0,095866	0,169639	0,716156	6,34E-05	0,007976	0,051216
0,56	0,106846301	0,136182368	0,699948	0,56	0,106917	0,135481	0,663433	7,07E-05	0,000701	0,036514
0,58	0,118707837	0,111443992	0,618135	0,58	0,118786	0,108266	0,601518	7,86E-05	0,003178	0,016617
0,6	0,131416278	0,087557476	0,511168	0,6	0,131503	0,090196	0,521053	8,7E-05	0,002639	0,009885
0,62	0,145000827	0,064676952	0,355958	0,62	0,145097	0,072162	0,400202	9,6E-05	0,007485	0,044244
0,64	0,159490688	0,043038038	0,091907	0,64	0,159596	0,049816	0,174853	0,000106	0,006778	0,082946
0,66	0,174915066	0,023055404	-0,50846	0,66	0,175031	0,025936	-1,03637	0,000116	0,002881	0,52791
0,68	0,191303162	0,005728853	-3,6939	0,68	0,19143	0,00861	-5,08451	0,000127	0,002881	1,390608
Total difference								0,002705	0,281998	6,873419

B PLOTS

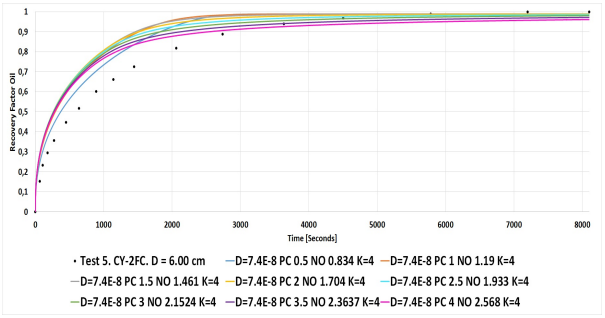

(a) *A figure showing the production curves of the different values for the changed No and PC values when the area under the diffusion coefficient curve is doubled. The PC curve has been multiplied with a given value.*

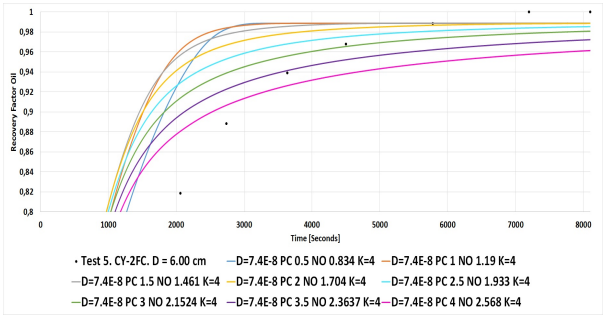

(b) *A zoomed in display of figure 33 that shows more detailed how the production curves varies towards the end.*

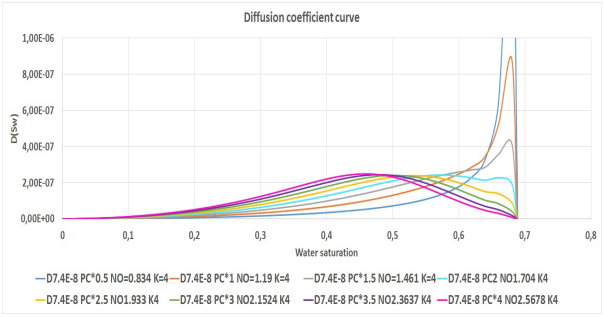

(c) *A figure showing the diffusion coefficient curve given by the different PC and No values when the total area underneath is doubled from the initial curve area. All of the curves have approximately the the same area underneath them.*

Figure 33

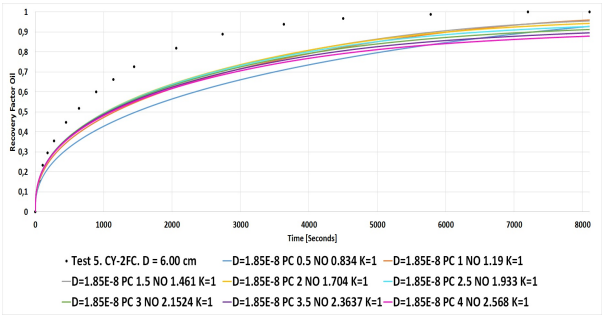

(a) *A figure showing the production curves of the different values for the changed No and PC values when the area under the diffusion coefficient curve is cut in half. The PC curve has been multiplied with a given value.*

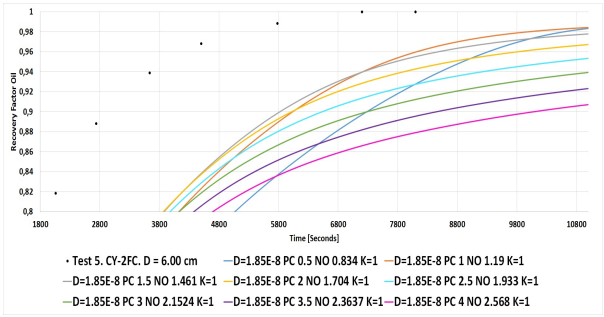

(b) *A zoomed in display of figure 34 that shows more detailed how the production curves varies towards the end.*

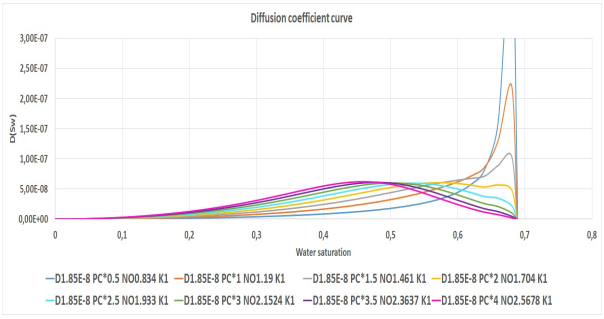

(c) *A figure showing the diffusion coefficient curve given by the different PC and No values when the total area underneath is cut in half from the initial curve area. All of the curves have approximately the the same area underneath them.*

Figure 34

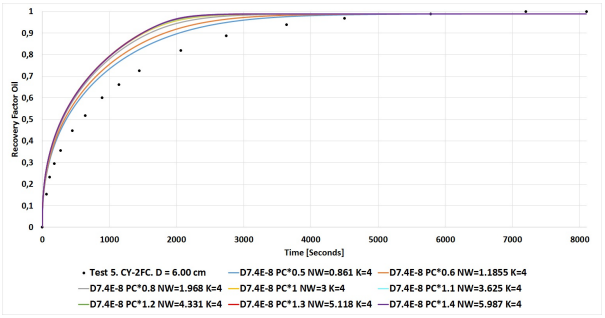

(a) *A figure showing the production curves of the different values for the changed Nw and PC values when the area under the diffusion coefficient curve is doubled. The PC curve has been multiplied with a given value.*

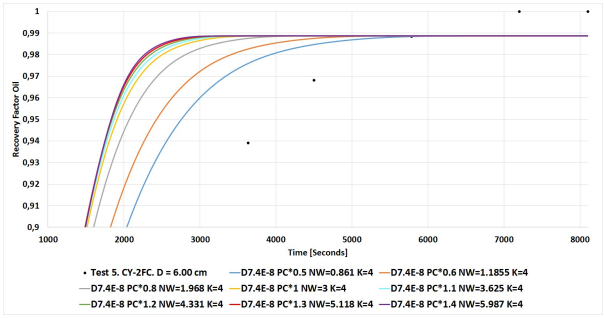

(b) *A zoomed in display of figure 35 that shows more detailed how the production curves varies towards the end.*

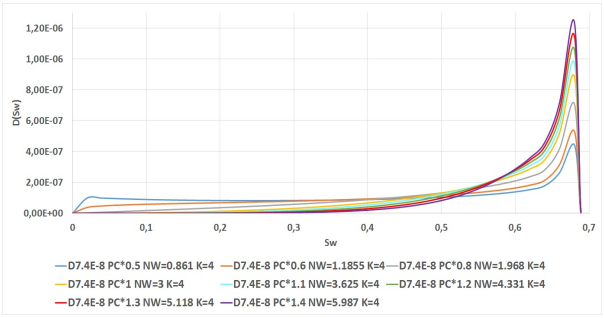

(c) *A figure showing the diffusion coefficient curve given by the different PC and Nw values when the total area underneath is doubled from the initial curve area. All of the curves have approximately the the same area underneath them.*

Figure 35

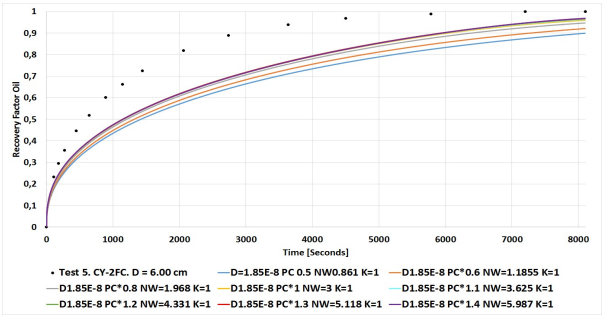

(a) *A figure showing the production curves of the different values for the changed Nw and PC values when the area under the diffusion coefficient curve is cut in half. The PC curve has been multiplied with a given value.*

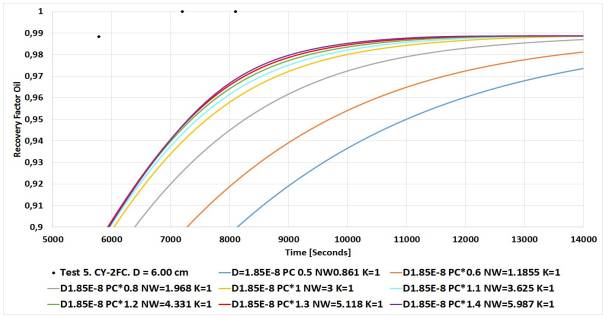

(b) *A zoomed in display of figure 36 that shows more detailed how the production curves varies towards the end.*

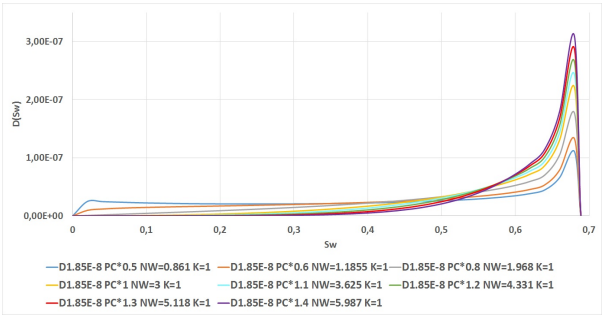

(c) *A figure showing the diffusion coefficient curve given by the different PC and Nw values when the total area underneath is cut in half from the initial curve area. All of the curves have approximately the the same area underneath them.*

Figure 36

C SIMULATOR

```
- -==============================================
- -SPONTANEOUS IMBIBITION OF WATER INTO OIL SATURATED POROUS MEDIA
- -==============================================

RUNSPEC

TITLE

SI OF WATER ONTO CHALK SATURATED WITH DECANE

–Keywords are written with capital letters comments with small.

DIMENS

– grid blocks in the r theta and z directions

40 20 40 /

–Only oil and water present in the model

OIL

WATER

–Using lab units (cm hours mD etc.)

LAB

EQLDIMS

2 100 20 1 20 /

TABDIMS

2 2 56 21 3 12 /

NUPCOL

4 /

–Radial geometry r theta and z

RADIAL

START

01 'JAN' 2016 /
```

NSTACK

50 /

–Unified summary files

UNIFOUT

UNIFIN

–NOSIM

GRIDOPTS

YES /

GRID ==========

INCLUDE

grid.DATA /

DTHETA

32000*18 /

DZ

32000*0.08 /

COORDSYS

1 40 COMP /

TOPS

800*0 800*0.08 800*0.16 800*0.24 800*0.32 800*0.4 800*0.48 800*0.56 800*0.64 800*0.72 800*0.8 800*0.88 800*0.96 800*1.04 800*1.12 800*1.2 800*1.28 800*1.36 800*1.44 800*1.52 800*1.6 800*1.68 800*1.76 800*1.84 800*1.92 800*2 800*2.08 800*2.16 800*2.24 800*2.32 800*2.4 800*2.48 800*2.56 800*2.64 800*2.72 800*2.8 800*2.88 800*2.96 800*3.04 800*3.12 /

- -The oil saturated cylindrical core sample is located in the

- - middle of a larger cylinder containing only water. Setting the

- - permeability in the whole region very high

–Permeability in r direction

PERMR

32000*100000 /

–Permeability in theta direction

PERMTHT

32000*100000 /

–Permeability in z direction

PERMZ

32000*100000 /

- - - - - -Permeability in the region representing the core sample

- - - - - - - - - -IX1-IX2-JY1-JY2-KZ1-KZ2

BOX

1 20 1 20 10 29 /

PERMR

8000*2 /

PERMTHT

8000*2 /

PERMZ

8000*2 /

ENDBOX

- - - - - - - - - - - -Porosity (= 0.95) in the region representing the fracture (outside the core sample)

PORO

32000*0.99 /

- - - - - -Porosity (0.49) in the area representing the core sample

- - - - - - - - - -IX1-IX2-JY1-JY2-KZ1-KZ2

BOX

1 20 1 20 10 29 /

PORO

8000*0.424 /

ENDBOX

MINPV

1E-10 /

INIT

- -close upper surface

- - - - - - - - - - - -IX1-IX2-JY1-JY2-KZ1-KZ2

BOX

1 20 1 20 9 9 /

MULTZ

400*0.0 /

ENDBOX

- -close lower surface

- - - - - - - - - - - -IX1-IX2-JY1-JY2-KZ1-KZ2

BOX

1 20 1 20 29 29 /

MULTZ

400*0.0 /

ENDBOX

- - Increase the pore volume outside the core sample to reduce boundary effects

BOX

21 40 1 20 10 29 /

MULTPV

8000*1000 /

BOX

1 40 1 20 1 9 /

MULTPV

7200*1000 /

BOX

1 40 1 20 30 40 /

MULTPV

8800*1000 /

PROPS ==========

SWOF

- -Relperm and cap pressure for water in the area representing the core sample

- - SW KRW KRO PCOW

0 0 1 12

0.02 4.86727E-06 0.965553197 8.290927431

0.04 3.89382E-05 0.931301527 7.227273352

0.06 0.000131416 0.897249849 6.643271266

0.08 0.000311505 0.8634033 6.242494513

0.1 0.000608409 0.829767321 5.937492507

0.12 0.00105133 0.796347687 5.690805881

0.14 0.001669473 0.76315054 5.483019227

0.16 0.002492042 0.730182425 5.302794573

0.18 0.003548239 0.697450335 5.142937719

0.2 0.00486727 0.664961756 4.998591296

0.22 0.006478336 0.632724729 4.866310382

0.24 0.008410642 0.600747914 4.743549486

0.26 0.010693391 0.569040666 4.628358794

0.28 0.013355788 0.537613125 4.519194266

0.3 0.016427035 0.506476328 4.414793035

0.32 0.019936336 0.475642334 4.314087683

0.34 0.023912895 0.445124382 4.216144217

0.36 0.028385916 0.414937078 4.120114407

0.38 0.033384602 0.385096629 4.02519634

0.4 0.038938156 0.355621131 3.930598609

0.42 0.045075783 0.32653094 3.835504218

0.44 0.051826686 0.297849139 3.739030012

0.46 0.059220069 0.269602149 3.640176336

0.48 0.067285134 0.241820551 3.53775907

0.5 0.076051087 0.214540196 3.430311206

0.52 0.08554713 0.187803769 3.315931193

0.54 0.095802466 0.161663056 3.192034847

0.56 0.106846301 0.136182368 3.054922379

0.58 0.118707837 0.111443992 2.89896301

0.6 0.131416278 0.087557476 2.71490402

0.62 0.145000827 0.064676952 2.485875229

0.64 0.159490688 0.043038038 2.175949224

0.66 0.174915066 0.023055404 1.684872199

0.68 0.191303162 0.005728853 0.461247591

0.688 0.198134784 0.000419294 -2.57547004

0.689 0.199 0 -2.955059744 /

- -Relperm and cap pressure for water in the fracture (Pcwo = 0)

- - SW KRW KRO PCWO

0.00000 0.00000 1.0000 0.00000

1.00000 1.00000 0.0000 0.00000 /

/

RSCONST

0 0.1 /

PVTW

10 1 4.4D-5 1.0 0 /

/

ROCK

10 4.2D-5 /

/

DENSITY

- - - OIL WATER GAS

0.731 0.9982 0.0097 /

/

PVDO

1.0 1.0 1

10 0.99999 1 /

/

REGIONS ==========

EQUALS

- - Core sample area is region 1

FIPNUM 1 1 20 1 20 10 29 /

SATNUM 1 1 20 1 20 10 29 /

- -Fracture system is region 2

FIPNUM 2 1 40 1 20 1 9 /

FIPNUM 2 1 40 1 20 30 40 /

FIPNUM 2 21 40 1 20 10 29 /

SATNUM 2 1 40 1 20 1 9 /

SATNUM 2 1 40 1 20 30 40 /

SATNUM 2 21 40 1 20 10 29 /

/

SOLUTION ==========

- -Defining the initial water saturation to 1.00 in the whole cylinder

SWAT

32000*1.00 /

- -Defining the initial water saturation in the core sample

- - - - - - - - - -IX1-IX2-JY1-JY2-KZ1-KZ2

BOX

1 20 1 20 10 29 /

SWAT

8000*0 /

ENDBOX

- -Defining the pressure in the whole model (core sample+fracture = 20.000 grid blocks))

equal to 1.00 bara

PRESSURE

32000*10.0 /

RPTSOL

RESTART=2 SOIL SWAT PRESSURE /

RPTRST

BASIC=6 NORST=1 FREQ=5 /

SUMMARY ==========

- -Region oil flux total between region 1 and 2

ROFT

1 2 /

/

–Region oil efficiency with respect to water

ROEIW

1 /

RWFT

1 2 /

/

BWSAT

1 1 19 /

2 1 19 /

3 1 19 /

4 1 19 /

5 1 19 /

6 1 19 /

7 1 19 /

8 1 19 /

9 1 19 /

10 1 19 /

11 1 19 /

12 1 19 /

13 1 19 /

14 1 19 /

15 1 19 /

16 1 19 /

17 1 19 /

18 1 19 /

19 1 19 /

20 1 19 /

/

BOSAT

1 1 19 /

2 1 19 /

3 1 19 /

4 1 19 /

5 1 19 /

6 1 19 /

7 1 19 /

8 1 19 /

9 1 19 /

10 1 19 /

11 1 19 /

12 1 19 /

13 1 19 /

14 1 19 /

15 1 19 /

16 1 19 /

17 1 19 /

18 1 19 /

19 1 19 /

20 1 19 /

/

RUNSUM

EXCEL

SCHEDULE ==========

RPTRST

BASIC=6 NORST=1 FREQ=5 /

MESSAGES

9* 10000 2* /

DRSDT

0 /

TUNING

0.001 0.25 0.005 0.005 /

/

50 1* 200 /

TSTEP

50*0.001 /

TSTEP

50*0.001 /

TSTEP

50*0.001 /

TSTEP

50*0.001 /

TSTEP

50*0.001 /

TSTEP

50*0.001 /

TSTEP

50*0.001 /

TSTEP

50*0.001 /

TSTEP

50*0.001 /

TSTEP

50*0.001 /

TSTEP

50*0.002 /

TSTEP

50*0.002 /

TSTEP

50*0.002 /

TSTEP

50*0.002 /

TSTEP

50*0.002 /

TSTEP

50*0.002 /

TSTEP

50*0.002 /

TSTEP

50*0.002 /

TSTEP

50*0.002 /

TSTEP

50*0.002 /

TSTEP

50*0.002 /

TSTEP

50*0.002 /

TSTEP

50*0.002 /

TSTEP

50*0.002 /

TSTEP

50*0.002 /

TSTEP

50*0.002 /

TSTEP

50*0.002 /

TSTEP

50*0.002 /

TSTEP

50*0.002 /

TSTEP

50*0.002 /

TSTEP

50*0.002 /

TSTEP

50*0.002 /

TSTEP

50*0.002 /

TSTEP

50*0.002 /

TSTEP

50*0.002 /

TSTEP

50*0.002 /

TSTEP

50*0.002 /

TSTEP

50*0.002 /

TSTEP

50*0.002 /

TSTEP

50*0.02 /

TSTEP

50*0.02 /

TSTEP

50*0.02 /

TSTEP

50*0.02 /

TSTEP

50*0.02 /

TSTEP

50*0.02 /

TSTEP

50*0.02 /

TSTEP

50*0.02 /

TSTEP

50*0.2 /

TSTEP

50*0.2 /

TSTEP

50*0.2 /

TSTEP

50*0.2 /

TSTEP

50*0.2 /

TSTEP

50*0.2 /

TSTEP

50*0.2 /

TSTEP

50*0.2 /

TSTEP

50*0.2 /

TSTEP

50*0.2 /

END

D GRID FOR 6CM CORE SIMULATION

The following include one of the 40 identical layers in the grid file:

NOECHO

INRAD

0.000000000001 /

–The grid is a large cylinder. The core sample containing oil is a smaller cylinder located inside the larger one.
–The area outside the core sample will be referred to as the fracture area.
–INCLUDE
– 'CYLINDER.FILLED' /

DR 0.00000001 0.960768923 0.397963518 0.305368148 0.257437257 0.226806776 0.205049 0.188562016 0.175509245 0.164841887 0.155911333 0.148291926 0.14169115 0.135900438 0.130766522 0.126173901 0.122033654 0.118276059 0.114845572 0.11169732 0.108794602 0.10610707 0.103609383 0.10128019 0.099101357 0.097057371 0.095134871 0.09332228 0.091609508 0.089987717 0.088449125 0.086986854 0.085594794 0.084267502 0.083000105 0.08178823 0.080627936 0.079515667 0.078448197 0.077422598 0.00000001 0.960768923 0.397963518 0.305368148 0.257437257 0.226806776 0.205049 0.188562016 0.175509245 0.164841887 0.155911333 0.148291926 0.14169115 0.135900438 0.130766522 0.126173901 0.122033654 0.118276059 0.114845572 0.11169732 0.108794602 0.10610707 0.103609383 0.10128019 0.099101357 0.097057371 0.095134871 0.09332228 0.091609508 0.089987717 0.088449125 0.086986854 0.085594794 0.084267502 0.083000105 0.08178823 0.080627936 0.079515667 0.078448197 0.077422598 0.00000001 0.960768923 0.397963518 0.305368148 0.257437257 0.226806776 0.205049 0.188562016 0.175509245 0.164841887 0.155911333 0.148291926 0.14169115 0.135900438 0.130766522 0.126173901 0.122033654 0.118276059 0.114845572 0.11169732 0.108794602 0.10610707 0.103609383 0.10128019 0.099101357 0.097057371 0.095134871 0.09332228 0.091609508 0.089987717 0.088449125 0.086986854 0.085594794 0.084267502 0.083000105 0.08178823 0.080627936 0.079515667 0.078448197 0.077422598 0.00000001 0.960768923 0.397963518 0.305368148 0.257437257 0.226806776 0.205049 0.188562016 0.175509245 0.164841887 0.155911333 0.148291926 0.14169115

0.135900438 0.130766522 0.126173901 0.122033654 0.118276059 0.114845572 0.11169732
0.108794602 0.10610707 0.103609383 0.10128019 0.099101357 0.097057371 0.095134871
0.09332228 0.091609508 0.089987717 0.088449125 0.086986854 0.085594794 0.084267502
0.083000105 0.08178823 0.080627936 0.079515667 0.078448197 0.077422598 0.00000001
0.960768923 0.397963518 0.305368148 0.257437257 0.226806776 0.205049 0.188562016
0.175509245 0.164841887 0.155911333 0.148291926 0.14169115 0.135900438 0.130766522
0.126173901 0.122033654 0.118276059 0.114845572 0.11169732 0.108794602 0.10610707
0.103609383 0.10128019 0.099101357 0.097057371 0.095134871 0.09332228 0.091609508
0.089987717 0.088449125 0.086986854 0.085594794 0.084267502 0.083000105 0.08178823
0.080627936 0.079515667 0.078448197 0.077422598 0.00000001 0.960768923 0.397963518
0.305368148 0.257437257 0.226806776 0.205049 0.188562016 0.175509245 0.164841887
0.155911333 0.148291926 0.14169115 0.135900438 0.130766522 0.126173901 0.122033654
0.118276059 0.114845572 0.11169732 0.108794602 0.10610707 0.103609383 0.10128019
0.099101357 0.097057371 0.095134871 0.09332228 0.091609508 0.089987717 0.088449125
0.086986854 0.085594794 0.084267502 0.083000105 0.08178823 0.080627936 0.079515667
0.078448197 0.077422598 0.00000001 0.960768923 0.397963518 0.305368148 0.257437257
0.226806776 0.205049 0.188562016 0.175509245 0.164841887 0.155911333 0.148291926
0.14169115 0.135900438 0.130766522 0.126173901 0.122033654 0.118276059 0.114845572
0.11169732 0.108794602 0.10610707 0.103609383 0.10128019 0.099101357 0.097057371
0.095134871 0.09332228 0.091609508 0.089987717 0.088449125 0.086986854 0.085594794
0.084267502 0.083000105 0.08178823 0.080627936 0.079515667 0.078448197 0.077422598
0.00000001 0.960768923 0.397963518 0.305368148 0.257437257 0.226806776 0.205049
0.188562016 0.175509245 0.164841887 0.155911333 0.148291926 0.14169115 0.135900438
0.130766522 0.126173901 0.122033654 0.118276059 0.114845572 0.11169732 0.108794602
0.10610707 0.103609383 0.10128019 0.099101357 0.097057371 0.095134871 0.09332228
0.091609508 0.089987717 0.088449125 0.086986854 0.085594794 0.084267502 0.083000105
0.08178823 0.080627936 0.079515667 0.078448197 0.077422598 0.00000001 0.960768923
0.397963518 0.305368148 0.257437257 0.226806776 0.205049 0.188562016 0.175509245
0.164841887 0.155911333 0.148291926 0.14169115 0.135900438 0.130766522 0.126173901
0.122033654 0.118276059 0.114845572 0.11169732 0.108794602 0.10610707 0.103609383

0.10128019 0.099101357 0.097057371 0.095134871 0.09332228 0.091609508 0.089987717
0.088449125 0.086986854 0.085594794 0.084267502 0.083000105 0.08178823 0.080627936
0.079515667 0.078448197 0.077422598 0.00000001 0.960768923 0.397963518 0.305368148
0.257437257 0.226806776 0.205049 0.188562016 0.175509245 0.164841887 0.155911333
0.148291926 0.14169115 0.135900438 0.130766522 0.126173901 0.122033654 0.118276059
0.114845572 0.11169732 0.108794602 0.10610707 0.103609383 0.10128019 0.099101357
0.097057371 0.095134871 0.09332228 0.091609508 0.089987717 0.088449125 0.086986854
0.085594794 0.084267502 0.083000105 0.08178823 0.080627936 0.079515667 0.078448197
0.077422598 0.00000001 0.960768923 0.397963518 0.305368148 0.257437257 0.226806776
0.205049 0.188562016 0.175509245 0.164841887 0.155911333 0.148291926 0.14169115
0.135900438 0.130766522 0.126173901 0.122033654 0.118276059 0.114845572 0.11169732
0.108794602 0.10610707 0.103609383 0.10128019 0.099101357 0.097057371 0.095134871
0.09332228 0.091609508 0.089987717 0.088449125 0.086986854 0.085594794 0.084267502
0.083000105 0.08178823 0.080627936 0.079515667 0.078448197 0.077422598 0.00000001
0.960768923 0.397963518 0.305368148 0.257437257 0.226806776 0.205049 0.188562016
0.175509245 0.164841887 0.155911333 0.148291926 0.14169115 0.135900438 0.130766522
0.126173901 0.122033654 0.118276059 0.114845572 0.11169732 0.108794602 0.10610707
0.103609383 0.10128019 0.099101357 0.097057371 0.095134871 0.09332228 0.091609508
0.089987717 0.088449125 0.086986854 0.085594794 0.084267502 0.083000105 0.08178823
0.080627936 0.079515667 0.078448197 0.077422598 0.00000001 0.960768923 0.397963518
0.305368148 0.257437257 0.226806776 0.205049 0.188562016 0.175509245 0.164841887
0.155911333 0.148291926 0.14169115 0.135900438 0.130766522 0.126173901 0.122033654
0.118276059 0.114845572 0.11169732 0.108794602 0.10610707 0.103609383 0.10128019
0.099101357 0.097057371 0.095134871 0.09332228 0.091609508 0.089987717 0.088449125
0.086986854 0.085594794 0.084267502 0.083000105 0.08178823 0.080627936 0.079515667
0.078448197 0.077422598 0.00000001 0.960768923 0.397963518 0.305368148 0.257437257
0.226806776 0.205049 0.188562016 0.175509245 0.164841887 0.155911333 0.148291926
0.14169115 0.135900438 0.130766522 0.126173901 0.122033654 0.118276059 0.114845572
0.11169732 0.108794602 0.10610707 0.103609383 0.10128019 0.099101357 0.097057371
0.095134871 0.09332228 0.091609508 0.089987717 0.088449125 0.086986854 0.085594794

0.084267502 0.083000105 0.08178823 0.080627936 0.079515667 0.078448197 0.077422598
0.00000001 0.960768923 0.397963518 0.305368148 0.257437257 0.226806776 0.205049
0.188562016 0.175509245 0.164841887 0.155911333 0.148291926 0.14169115 0.135900438
0.130766522 0.126173901 0.122033654 0.118276059 0.114845572 0.11169732 0.108794602
0.10610707 0.103609383 0.10128019 0.099101357 0.097057371 0.095134871 0.09332228
0.091609508 0.089987717 0.088449125 0.086986854 0.085594794 0.084267502 0.083000105
0.08178823 0.080627936 0.079515667 0.078448197 0.077422598 0.00000001 0.960768923
0.397963518 0.305368148 0.257437257 0.226806776 0.205049 0.188562016 0.175509245
0.164841887 0.155911333 0.148291926 0.14169115 0.135900438 0.130766522 0.126173901
0.122033654 0.118276059 0.114845572 0.11169732 0.108794602 0.10610707 0.103609383
0.10128019 0.099101357 0.097057371 0.095134871 0.09332228 0.091609508 0.089987717
0.088449125 0.086986854 0.085594794 0.084267502 0.083000105 0.08178823 0.080627936
0.079515667 0.078448197 0.077422598 0.00000001 0.960768923 0.397963518 0.305368148
0.257437257 0.226806776 0.205049 0.188562016 0.175509245 0.164841887 0.155911333
0.148291926 0.14169115 0.135900438 0.130766522 0.126173901 0.122033654 0.118276059
0.114845572 0.11169732 0.108794602 0.10610707 0.103609383 0.10128019 0.099101357
0.097057371 0.095134871 0.09332228 0.091609508 0.089987717 0.088449125 0.086986854
0.085594794 0.084267502 0.083000105 0.08178823 0.080627936 0.079515667 0.078448197
0.077422598 0.00000001 0.960768923 0.397963518 0.305368148 0.257437257 0.226806776
0.205049 0.188562016 0.175509245 0.164841887 0.155911333 0.148291926 0.14169115
0.135900438 0.130766522 0.126173901 0.122033654 0.118276059 0.114845572 0.11169732
0.108794602 0.10610707 0.103609383 0.10128019 0.099101357 0.097057371 0.095134871
0.09332228 0.091609508 0.089987717 0.088449125 0.086986854 0.085594794 0.084267502
0.083000105 0.08178823 0.080627936 0.079515667 0.078448197 0.077422598 0.00000001
0.960768923 0.397963518 0.305368148 0.257437257 0.226806776 0.205049 0.188562016
0.175509245 0.164841887 0.155911333 0.148291926 0.14169115 0.135900438 0.130766522
0.126173901 0.122033654 0.118276059 0.114845572 0.11169732 0.108794602 0.10610707
0.103609383 0.10128019 0.099101357 0.097057371 0.095134871 0.09332228 0.091609508
0.089987717 0.088449125 0.086986854 0.085594794 0.084267502 0.083000105 0.08178823
0.080627936 0.079515667 0.078448197 0.077422598 0.00000001 0.960768923 0.397963518

0.305368148 0.257437257 0.226806776 0.205049 0.188562016 0.175509245 0.164841887 0.155911333 0.148291926 0.14169115 0.135900438 0.130766522 0.126173901 0.122033654 0.118276059 0.114845572 0.11169732 0.108794602 0.10610707 0.103609383 0.10128019 0.099101357 0.097057371 0.095134871 0.09332228 0.091609508 0.089987717 0.088449125 0.086986854 0.085594794 0.084267502 0.083000105 0.08178823 0.080627936 0.079515667 0.078448197 0.077422598 ——-